

ABSTRACT

Title of Thesis: INVESTIGATING THE DIABETIC BRAIN:
THE EFFECTS OF PIOGLITAZONE AND
INSULIN ON THE CELLULAR PROCESSES
AND PATHOLOGY OF ALZHEIMER'S
DISEASE

Tanya Bagheri, Vincent Bennett, Annelise Buck,
Kelles Gordge, Ilana Green, Eric Kang, Nahye
Kim, Caroline McCue, Unnati Mehta, Shannon
Morken, Mayumi Rezwani, Ashley Zachery

Directed By: Dr. Kara Duffy, PhD,
Center for Biomolecular Therapeutics
University of Maryland School of Medicine

Alzheimer's disease (AD) is the sixth leading cause of death in the US. Some researchers refer to AD as "Type III Diabetes" because of reported glucose metabolism dysfunction. Preclinical studies suggest increasing insulin decreases AD pathology, although the mechanism remains unclear. To sensitize insulin signaling, this study activated Peroxisome Proliferator-Activated Receptor Gamma using intranasal co-administration of pioglitazone (PGZ) and insulin. This method targeted the site of action to reduce peripheral effects and to maximize impact in transgenic mice expressing AD pathology. Data from GC-MS fluxomics analysis suggested that PGZ+Insulin increased glucose metabolism in the brain. Immunohistochemistry with relevant antibodies was used to identify AD pathological markers in the subiculum, indicating that PGZ+Insulin decreased pathology compared to Insulin and Saline. This suggests that increasing glucose uptake in the brain alleviated AD pathology, further clarifying the role of insulin signaling in AD pathology.

INVESTIGATING THE DIABETIC BRAIN: THE EFFECTS OF PIOGLITAZONE
AND INSULIN ON THE CELLULAR PROCESSES AND PATHOLOGY OF
ALZHEIMER'S DISEASE

By

Team Brain Blast

Tanya Bagheri, Vincent Bennett, Annelise Buck, Kelles Gordge, Ilana Green, Eric Kang,
Nahye Kim, Caroline McCue, Unnati Mehta, Shannon Morken, Mayumi Rezwan, Ashley
Zachery

Thesis submitted in partial fulfillment of the Gemstone Program
University of Maryland
2016

Advisory Committee:

Dr. Kara Duffy, Faculty Mentor
Dr. Ricardo C. Araneda
Dr. William T. Regenold
Dr. Matthew Roesch
Dr. Nam Sun Wang

© Copyright by

Tanya Bagheri, Vincent Bennett, Annelise Buck, Kelles Gordge, Ilana Green, Eric Kang, Nahye Kim, Caroline McCue, Unnati Mehta, Shannon Morken, Mayumi Rezwan, Ashley Zachery

Dr. Kara Duffy

2016

Preface

This thesis is submitted as part of the Gemstone program, a four-year interdisciplinary honors program at the University of Maryland. In the Gemstone program, students create and complete their own research projects in teams led by a faculty member. The purpose of this rigorous program is to allow students to develop the skills to research problems relevant to society, foster teamwork and leadership, and provide a supporting community of dedicated students.

Team Brain Blast is made up of 12 undergraduate students with majors ranging from International Business to Mechanical Engineering to Physiology and Neurobiology. Dr. Kara Duffy serves as the team mentor and a researcher at the University of Maryland School of Medicine's Center for Bimolecular Therapeutics.

Dedication

We were the last gemstone team of our cohort to receive a mentor because it was difficult to find someone who specialized in our research area of interest. Although he did not have much background in our research area, Dr. B stepped up and offered to be our mentor because he had had such a great experience mentoring a previous gemstone team, and was excited to learn along with us. Dr. B was integral in the development of our project. He was a brilliant scientist, excited to learn about a new area. Beyond his intelligence, Dr. B was an incredible mentor figure, as well as friend, to each and every one of us. He showed genuine care and interest in all of our lives, and loved to learn about our academic endeavors, as well as extracurricular interests. He also liked to share gossip with us and we would often have to focus him at our meetings to talk about science. It is clear that Dr. B made friends everywhere he went because many of his colleagues were happy to help our team.

It was because of Dr. B that we were able to meet our current mentor Dr. Kara Duffy, who had agreed to be our team expert in the beginning stages of our project. In dealing with Dr. B's passing, our team again found ourselves lucky enough to have someone step up and become our mentor even when the circumstances were not easy—and for that, we are incredibly grateful to Kara. We could not have achieved finishing our research without her or anyone else who had helped us along the way—and the fact that so many of Dr. B's colleagues had gone out of their way to help us after his passing is a true testament to his character and the genuine relationships he had with them.

In team meetings, we often reminisce about our memories with Dr. B, or ask “what would Dr. B think about this?” It is clear that his presence remains all throughout our project, and for that, we dedicate our research to Dr. Brian Bequette. We hope we made him proud.

Acknowledgements

We would like to thank Dr. Brian Bequette for providing us with inspiration for not only our research, but for our endeavors in all aspects of our student lives as well. We would also like to give special thanks to Dr. Kara Duffy for her guidance and support during the challenging progression of our project. Dr. Kristan Skendall, Dr. Frank Coale, and the rest of the Gemstone staff have provided us with endless support in our research and team-building endeavors. Nedelina Tchangalova has provided us with excellent input on the content and structure of our writing. Many thanks to Dr. Thomas Castonguay for providing us with both guidance and materials when needed. Thank you to Dr. Danna Zimmer for allowing us the use of her lab space, equipment, and materials. Thank you to Leslie Juengst for going above and beyond in helping us decide the fluxomics route that we ultimately utilized. Thank you to Dr. Yue Li for guiding and supervising us through the process of completing our fluxomics tests. Thank you to all of our Launch UMD donors who made our project possible. Thank you to the Animal Science Department, especially Dr. Angela Black and Tikina Smith, for supporting us in our animal research. Without any of these individuals, our research would not be where it is today.

Table of Contents

| | |
|---|------|
| Preface..... | ii |
| Dedication..... | iii |
| Acknowledgements..... | v |
| Table of Contents..... | vi |
| List of Figures..... | viii |
| List of Abbreviations..... | ix |
| Chapter 1: Introduction..... | 1 |
| 1.1 Problem Description and Motivation..... | 1 |
| 1.2 Characterization of Alzheimer’s Disease..... | 1 |
| 1.3 Effects on Society..... | 3 |
| 1.3 Risk Factors and Diagnosis Of Alzheimer’s Disease..... | 4 |
| 1.3.1 Risk Factors..... | 4 |
| 1.3.2 Types of Alzheimer’s Disease..... | 5 |
| 1.3.3 Diagnosis..... | 6 |
| 1.4 Experimental Approach..... | 8 |
| 1.5 Research Questions and Hypothesis..... | 9 |
| Chapter 2: Literature Review..... | 10 |
| 2.1 Pathology of Alzheimer’s Disease..... | 10 |
| 2.1.1 Amyloid Beta Plaques..... | 10 |
| 2.1.2 Neurofibrillary Tangles..... | 11 |
| 2.1.3 Inflammation..... | 12 |
| 2.1.4 Apoptosis..... | 13 |
| 2.1.5 Diminished Cerebral Glucose Metabolism..... | 17 |
| 2.2 Glucose Metabolism..... | 18 |
| 2.2.1 Glucose Metabolism in the Brain..... | 19 |
| 2.3 Insulin Signaling Pathway..... | 21 |
| 2.3.1 PPAR γ | 24 |
| 2.4 Current Alzheimer’s Disease Research: Thiazolidinediones and Insulin..... | 27 |
| 2.4.1 Thiazolidinediones and Alzheimer’s Disease..... | 28 |
| 2.4.2 Insulin and Alzheimer’s Disease..... | 31 |
| 2.4.3 Intranasal Administration of Insulin and Thiazolidinediones..... | 32 |
| Chapter 3: Research Strategy..... | 34 |
| 3.1 Intranasal Method..... | 34 |
| 3.2 Pilot Study..... | 35 |
| 3.3 Experimental Design: Main Study..... | 36 |
| 3.3.1 Mouse Model..... | 36 |
| 3.3.2 Subiculum..... | 38 |
| 3.3.3 Treatment Groups..... | 39 |
| 3.3.4 Study Phases..... | 39 |
| 3.3.5 Immunohistochemistry Antibodies..... | 41 |
| 3.3.6 Fluxomics..... | 41 |

| | |
|---|----|
| Chapter 4: Methodology | 43 |
| 4.1 Animal Care | 43 |
| 4.2 Intranasal Administration..... | 43 |
| 4.3 Sample Collection..... | 44 |
| 4.4 Immunohistochemistry | 44 |
| 4.5 Image Analysis..... | 45 |
| 4.6 Statistics | 46 |
| 4.7 Luminescence Assay..... | 47 |
| 4.8 Fluxomics..... | 47 |
| Chapter 5: Results | 49 |
| 5.1 Immunohistochemistry | 49 |
| 5.1.1 6E10 (A β plaque)..... | 49 |
| 5.1.2 Iba1 (Inflammation)..... | 52 |
| 5.1.3 AT8 (PHF-tau)..... | 56 |
| 5.2 Luminescence Assays | 58 |
| 5.3 Fluxomics..... | 59 |
| Chapter 6: Discussion | 60 |
| Chapter 7: Conclusion..... | 67 |
| 7.1 Future Directions | 69 |
| Appendices..... | 72 |
| Appendix A: Pilot Results | 72 |
| Appendix B: Animal Care Training..... | 74 |
| Appendix C: Intranasal Insulin Method..... | 76 |
| Appendix D: In Depth Calculation of Intranasal PGZ Doses..... | 78 |
| Appendix E: Immunohistochemistry Protocols | 80 |
| Appendix F: Fluxomics Protocol | 83 |
| Appendix G: Caspase 3 and 9..... | 85 |
| Glossary | 86 |
| Bibliography | 92 |

List of Figures

| | |
|--|----|
| Figure 1: 2015 Distribution of AD Expenditure. | 4 |
| Figure 2: Apoptosis Signaling Pathway. | 15 |
| Figure 3: APP Processing. | 16 |
| Figure 4: Glucose Transport in the CNS. | 21 |
| Figure 5: Simplified ISP. | 23 |
| Figure 6: Simplified ISP Including PPAR γ . | 25 |
| Figure 7: The Insulin-dependent Mechanism of PPAR γ Gene Transcription. | 26 |
| Figure 8: Simplified ISP Including PPAR γ and PGZ. | 29 |
| Figure 9: Anatomical Features of a Mouse Brain. | 38 |
| Figure 10: Phases in Main Study. | 40 |
| Figure 11: Amyloid Deposition Phase I. | 50 |
| Figure 12: Amyloid Deposition Phase II. | 51 |
| Figure 13: Amyloid Deposition Phase III. | 52 |
| Figure 14: Iba1 Activated Microglia Ranking Phase I. | 53 |
| Figure 15: Iba1 Activated Microglia Ranking Phase II. | 54 |
| Figure 16: Iba1 Activated Microglia Ranking Phase III. | 55 |
| Figure 17: AT8 PHF-tau Phase I. | 56 |
| Figure 18: AT8 PHF-tau Phase II. | 57 |
| Figure 19: AT8 PHF-tau Phase III. | 58 |
| Figure 20: The Proposed Mechanisms by which the Insulin Treatment Ameliorates AD Pathology. | 68 |
| Figure 21: The Proposed Mechanisms by which the TZD Treatment Ameliorates AD Pathology. | 69 |
| Figure 22: Glucose Metabolism. | 73 |
| Figure 23: Intranasal Grip. | 77 |

List of Abbreviations

3x-Tg-AD – Triple Transgenic AD
AD – Alzheimer’s disease
Akt1 – Protein Kinase B
Akt2 – Protein Kinase B
ANSC – Animal Sciences
AP-1 – Activator Protein-1
ApoE – Apolipoprotein E
APP – Amyloid Precursor Protein
ATP – Adenosine Triphosphate
A β – Amyloid Beta
BACE1 – Beta-Secretase 1
BBB – Blood Brain Barrier
CAP – Cbl-Associated Protein
CARF – Central Animal Resource Facility
Cdk5 – Cyclin-Dependent Kinase 5
CNS – Central Nervous System
CT – Computerized Tomography
DCGM – Diminished Cerebral Glucose Metabolism
DISC – Death-Inducing Signaling Complex
GC-MS – Gas Chromatography- Mass Spectrometry
GLUT1 – Glucose Transporter 1
GLUT3 – Glucose Transporter 3
GLUT4 – Glucose Transporter 4
IACUC – Institutional Animal Care and Use Committee
Iba1 – Ionizing Calcium-Binding Adaptor Molecule 1
IDE – Insulin Degrading Enzyme
IHC – Immunohistochemistry
IL-6 – Interleukin-6
IPAc – Di-O-Isopropylidene Acetate
IR – Insulin Receptor
IRS1 – Insulin Receptor Substrate 1
ISP – Insulin Signaling Pathway
JNK – c-Jun N-Terminal Kinase
LTP – Long-Term Potentiation
M2 – Microglia in Anti-Inflammatory State
MCI – Mild Cognitive Impairment
mRNA – Messenger Ribonucleic Acid
MRI- Magnetic Resonance Imaging
NCD – Neurocognitive Disorder
NFT – Neurofibrillary Tangle
NMDA – N-Methyl-D-Aspartate
NR – Nuclear Receptor
PBS – Phosphate Buffered Saline
PDK1 – Phosphoinositide Dependent Protein Kinase-1

PET – Positron Emission Tomography
PGZ – Pioglitazone
PHF-tau – Paired Helical Filament Tau
PI₃K – Phosphoinositide 3-Kinase
PKC ζ – Protein Kinase C Zeta
PPAR γ – Peroxisome Proliferator-Activated Receptor Gamma
PPRE – PPAR Response Element
RGZ – Rosiglitazone
RIU – Relative Intensity Units
RXR – Retinoid X Receptor
SEM – Standard Error of the Mean
SNIFF – Study of Nasal Insulin to Fight Forgetfulness
T2D – Type II Diabetes
TNF α – Tumor Necrosis Factor Alpha
TZD – Thiazolidinedione

Chapter 1: Introduction

1.1 Problem Description and Motivation

Alzheimer's Disease (AD) is a major neurocognitive disorder (NCD) that progressively destroys memory and other cognitive functions. AD was named after Dr. Alois Alzheimer, who first characterized the disease in 1906. AD is the most common form of major NCD and currently impacts the lives of over five million Americans. It is now the sixth leading cause of death in the United States, mostly affecting people 65 years of age and older (Alzheimer's Association, 2015).

Although there are pharmaceutical approaches to alleviate AD symptoms, effective options for long-term treatment of AD and methods to prevent its onset have yet to be discovered, for the complete mechanism of AD is unclear. AD medications currently available help temporarily compensate for dysregulation of neurochemicals involved in the disease, but there is currently no modality that reverses or completely halts disease progression (Alzheimer's Association, 2015). Though the exact cause of AD remains unknown, extensive research is being conducted to understand the mechanisms of AD and to search for novel treatments.

1.2 Characterization of Alzheimer's Disease

The Diagnostic and Statistical Manual of Mental Disorders-5 characterizes major NCD, formerly referred to as "dementia," by a decline of performance in attention, language, social cognition, learning, and memory that interferes with

everyday activities and cannot be explained by another mental disorder (American Psychiatric Association, 2013). Some major NCDs are considered reversible, meaning symptoms associated with these pathologies can be alleviated after treatment, but AD is currently irreversible and progressively worsens with time (Tripathi & Vibha, 2009).

Cognitive symptoms of AD are characterized by the “4 A’s” of Alzheimer’s: amnesia, aphasia, apraxia, and agnosia (Alzheimer’s Foundation of America, 2016). Amnesia is a loss of memory, and occurs as deterioration, first, of short term memory and then of long term memory as the disease progresses. The first “A,” amnesia, is a large contributing factor to the development of the other three “A’s.” Aphasia is the inability to communicate effectively, which manifests in individuals suffering from AD as difficulty thinking of the appropriate words for communication. Apraxia is the inability to perform pre-programmed motor tasks, and in AD, is caused by memory loss of motor skills learned during development. Agnosia is the inability to properly interpret sensory signals. In the context of AD, this emerges in different ways as the disease progresses, from no longer recognizing a person’s face to no longer understanding the meaning of the sensation of a full bladder. These symptoms result in the inability to complete daily activities without significant assistance. In addition to these cognitive symptoms, AD can also develop with major psychiatric symptoms, including personality changes, depression, hallucinations, and delusions. Underlying these cognitive and psychiatric symptoms are the pathological hallmarks of AD in the brain: aggregated protein plaques and tangles, hyperactive cell death, and failure to

meet the metabolic demands of healthy brain functioning (De La Monte & Wands, 2008).

1.3 Effects on Society

AD not only affects its patients, but also takes a substantial toll on the families of patients. In 2014, more than 15 million family members and other unpaid caregivers provided an estimated 17.9 billion hours of care to people with AD and varying NCDs, a contribution valued at more than \$217.7 billion (Alzheimer's Association, 2015).

AD carries heavy financial, physical, and mental burdens for caregivers and family members. As of 2015, the collective care costs for AD individuals in the United States totaled \$226 billion, and approximately 18% of that cost had to be covered as out-of-pocket, not reimbursed by insurance, expenses for the families of AD patients (Figure 1). By 2050, these costs are expected to grow to six times that amount, or to approximately \$1.1 trillion (Alzheimer's Association, 2015). If the distribution remains unchanged, families will need to cover \$330 billion of care costs. In addition, a 2015 survey reflected the significant physical and mental burdens on caretakers: 60% of caregivers reported high to very high stress levels, and 40% reported having depression (Alzheimer's Association, 2015). It is clear that AD's destruction reaches far beyond the brains of those afflicted.

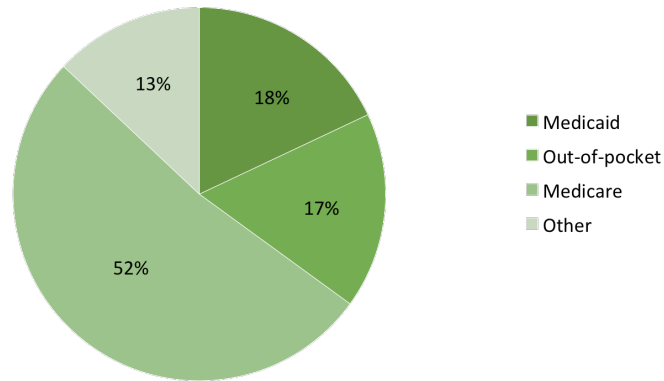


Figure 1. 2015 Distribution of AD Expenditure. *Costs of AD in America totaled \$226 billion in 2015. Approximately \$158 billion of the cost associated with AD care is covered by Medicare and Medicaid, while the remaining coverage falls to caregivers and totals a 68 billion dollar financial burden.* Information from 2015 Alzheimer’s Disease Facts and Figures (2015). Created by I. Green.

1.3 Risk Factors and Diagnosis Of Alzheimer’s Disease

1.3.1 Risk Factors

Ninety-six percent of Americans with AD are 65 years of age or older, highlighting the importance of age as a risk factor for AD (Alzheimer’s Association, 2015). The risk of developing AD doubles every five years after the age of 65. In addition to age, lifestyle and genetics are also risk factors (National Institutes of Health, 2016). Smoking, obesity, lack of mental activity, and head trauma increase the likelihood of developing AD (National Institutes of Health, 2016). Type 2 diabetes mellitus (T2D) is yet another factor that increases the risk of developing this

disease by 50-60% (Chami et al., 2016; Mittal & Katare, 2016). The comorbidity of AD and T2D appears to be more than just coincidence.

Studies have been conducted since the 1990s to assess the relationship between AD and T2D. In the majority of conducted studies, researchers found that increased body mass index and insulin resistance, both risk factors/indicators of T2D, were associated with increased risk of AD (Hammaker, 2014). Compared to the general population, patients with T2D have a 50-150% increased risk for AD (Li, Song, & Leng, 2015). Repeated evidence of this relationship fueled a group of researchers at Brown University to begin referring to AD as “Type III Diabetes” (Hammaker, 2014). Both of these diseases involve glucose uptake deficits (De La Monte & Wands, 2008). Even though AD involves aberrations in glucose metabolism in the brain, while T2D functions in the periphery, researchers hypothesize an interplay between these diseases (Moroz, Tong, Longato, Xu, & De La Monte, 2008; Sebastiao, Candeias, Santos, Oliveira, Moreira & Duarte, 2014). This research project focuses on the theory that AD is at least partially caused by improper glucose uptake.

1.3.2 Types of Alzheimer’s Disease

The genetic risk factors of AD vary in strength depending on the subtype of AD. AD is characterized by two subtypes: familial and sporadic. Familial AD is heavily dependent on genetics, as it is an autosomal dominant disease that is inherited through at least one of three known major genetic loci (Rossor, Fox, Freeborough & Harvey, 1996). In contrast, genetic makeup does not contribute largely to sporadic

AD, although certain genetic phenotypes may increase one's susceptibility for the disease (Trippi, 2001).

Familial AD is the hereditary subtype of AD and as a result, more is known about its pathological development. Genetic mutations that cause familial AD occur on the APP gene on Chromosome 21, the Presenilin 1 gene on Chromosome 14, or the Presenilin 2 gene on Chromosome 1 (Ryan & Rossor, 2010). These three genes account for nearly all familial AD cases. Additional research is being conducted to determine all of the genetic sites associated with familial AD pathology (Cruts, Theuns & Van Broeckhoven, 2012). Although familial AD accounts for a minority of AD cases, it provides a useful way to study AD.

While it is easier to study familial AD than sporadic, sporadic AD accounts for over 99.5% of all AD cases (Cruts et al., 2012). This AD subtype is characterized by later onset and is not strongly associated with certain genotypes (Trippi, 2001). While not causative, genetics does play a role in regard to risk. Carriers of the Apolipoprotein E (ApoE- ϵ 4) allele are more likely to develop AD than those with a different version of ApoE- ϵ 4. Individuals with the ApoE- ϵ 4 isoform represent roughly 20% of the population but make up 35-50% of sporadic AD cases (Hamerman, 2007; Alzheimer's Association, 2015).

1.3.3 Diagnosis

Dr. Alzheimer characterized the plaques and tangles that define AD, specifically referred to as amyloid-beta ($A\beta$) plaques and neurofibrillary tangles (NFTs) made of tau paired helical filaments (PHF-tau), using staining methods similar to what are still used in research today. Markers for these brain abnormalities

are necessary for an official diagnosis of AD and can only be definitively determined post-mortem. While post-mortem analysis is necessary for an official diagnosis, methods used to obtain information about AD biomarkers during life, such as analyzing cerebrospinal fluid, or brain scans such as positron emission tomography (PET), magnetic resonance imaging (MRI), and computerized tomography (CT), can help understand the progression of the disease up until death (Cipriani, Dolciotti, Picchi & Bonuccelli, 2010).

Characterizing AD in a living patient is important for both medical management as well as research, and as a result, three stages of “probable AD” diagnosis are incorporated in the DSM-5. These three stages, in order of increasing severity, are preclinical, mild NCD, and major NCD due to AD (Alzheimer’s Association & NIA, 2011). The purpose of the diagnosis of preclinical AD is to measure early biomarker changes, in the absence of cognitive or behavioral symptoms, in someone who is predicted to have AD based on a family history or abundance of risk factors. A diagnosis of mild NCD due to AD is a characterization of mild decline in cognitive and behavioral function that is not severe enough to affect independent functioning in everyday life. With this diagnosis, evidence of biomarkers is highly encouraged to avoid an inaccurate diagnosis. Finally, a diagnosis of major NCD due to AD is considered a complete manifestation of AD, involving severe behavioral and cognitive impairments that compromise a person’s ability to function independently in everyday life. Although the psychiatric symptoms are sufficient for diagnosis, biomarker evidence helps increase diagnostic certainty (Alzheimer’s Association & NIA, 2011).

1.4 Experimental Approach

As previously discussed, a recent focus of AD research has been the connection between AD and T2D. Both diseases involve deficits in glucose transport from the blood into cells for metabolism, which is mediated by insulin. For this reason, researchers are making connections between T2D and AD with existing knowledge about T2D treatment and intracellular processes. To investigate the insulin signaling pathway (ISP) in AD, researchers use various drugs normally used for treatment of T2D. One such class of drugs is the Thiazolidinediones (TZDs), which agonize downstream targets of the ISP to explore the compromised metabolic component of AD pathology (Leibiger, Leibiger & Berrgren, 2008; Zolezzi & Inestrosa, 2013). While both insulin and TZDs have been used to investigate AD, the combined effects of the two have not been studied. Doing so may provide useful since insulin facilitates cellular glucose uptake and TZDs agonize targets within the ISP to enhance insulin's effects (Leibiger, Leibiger & Berrgren, 2008; Zolezzi & Inestrosa, 2013).

Since the body's blood brain barrier (BBB) only allows approximately 18% of pioglitazone (PGZ), a type of TZD, to cross from the periphery into the central nervous system (CNS) when administered orally, it is advantageous to deliver the drug directly to the brain where AD pathology occurs (Maeshiba et al., 1997). In order to achieve this goal, drugs can be delivered using an intranasal delivery method (Talegaonkar & Mishra, 2004).

Intranasal delivery of insulin to the brain has been performed in the context of AD research and clinical trials as an AD treatment (Freiherr et al., 2013). A clinical

trial, the Study of Nasal Insulin to Fight Forgetfulness (SNIFF), for intranasal insulin therapy is currently underway to test the effects of insulin nasal spray in adults with mild cognitive impairment or AD (University of Southern California, 2016).

However, TZDs have never been administered in this or any other way to selectively target the CNS. This study successfully executed the first intranasal administration of PGZ in conjunction with insulin to research AD pathology.

1.5 Research Questions and Hypothesis

This research aimed to determine the downstream metabolic components of the ISP that are aberrant in AD by modulating the activity of this pathway with intranasal insulin and PGZ during the onset of AD development. Pathological markers of AD and glucose metabolism in the brain were measured to investigate aberrations in the ISP in the context of AD. A transgenic mouse model expressing AD pathology was used to answer the following questions:

1. Does intranasal administration of PGZ and insulin sensitize insulin signaling to increase glucose metabolism?
2. Will three weeks of PGZ and insulin treatment reduce AD pathology?
3. Do reductions in pathology persist two weeks after completing the dosing regimen?

The combined treatment of insulin and PGZ was hypothesized to create long lasting reductions in AD pathology as a result of improved glucose uptake.

Chapter 2: Literature Review

2.1 Pathology of Alzheimer's Disease

The AD brain is characterized by a prolonged immune response and increased apoptosis (Mandrekar & Landreth, 2010). In addition, A β peptides and PHF-tau protein aggregates that form A β plaques and NFTs precede the cognitive and behavioral symptoms of AD (Wang et al., 2015). This protein aggregation occurs in various parts of the brain, but the majority of severe pathology is concentrated in the hippocampus, the region in the brain predominantly responsible for learning and memory. Certain subregions of the hippocampus are also associated with increased AD pathology (Willette, Modanlo & Kapogiannis, 2015). Plaques first appear in the subiculum and then spread to the rest of the brain (George et al., 2014). As the disease progresses, pathology spreads primarily to areas in the limbic system, such as the hippocampus and amygdala, which contributes to memory loss, disorientation, and behavioral changes (U.S. Department of Health and Human Services, n.d.).

2.1.1 Amyloid Beta Plaques

The starting point of AD progression is unknown, but several competing theories aim to explain the progression of the disease. The amyloid cascade hypothesis, which is of particular relevance to this study, cites the imbalance between production and clearance of both internal and external A β plaques as the primary cause of AD (Zou et al., 2015). This hypothesis suggests that the formation of A β plaques is the primary event in AD pathogenesis and is caused by the aggregation of the peptides, specifically peptides A β ₄₀ and A β ₄₂, caused by improper cleavage of

natural cellular proteins. This pathogenic form causes the aggregation of peptides and yields a cascade of negative effects contributing to AD (Tong, Lou & Wang, 2015; Hardy & Selkoe, 2002). These peptides are byproducts of altered amyloid precursor protein (APP) proteolysis. APP is an integral membrane protein concentrated around the synapses of neurons that, when functioning properly, serves as a regulator of synapse formation, neural plasticity, and iron export (Turner, O'Connor, Tate & Abraham, 2003). APP is normally broken down by α - and γ -secretases to produce sAPP α , which has neurotrophic and neuroprotective effects (Zhang, Ma, Zhang & Xu, 2012). However, in AD, there is an altered pathway in which APP is cleaved by β -secretase, resulting in A β protein formation. The tertiary structure of A β proteins can form dangerous oligomers that induce other A β proteins to aggregate, ultimately forming large A β plaques. These resulting A β plaques are not only toxic to neurons, but also yield indirect effects on AD pathology. These effects include triggering cascades of neuroinflammation, oxidative stress, tau hyperphosphorylation, and tangle formation, ultimately resulting in major NCD (Collins-Praino et al., 2014).

2.1.2 Neurofibrillary Tangles

In addition to the improperly cleaved proteins that contribute to A β plaques, another major contributor to AD pathology is the hyperphosphorylation of the structural protein tau. Tau, a soluble protein found in neurons of the CNS, binds to and stabilizes microtubules, aiding the transport of nutrients, neurotransmitters, and cellular materials down the axon of a cell. Tau can also act as a protein scaffold and participate in signal transduction cascades (Peric & Annaert, 2015). Normally, tau is phosphorylated to fine-tune its function, but in AD, tau is hyperphosphorylated. The

hyperphosphorylated version of tau is referred to as PHF-tau and causes the protein to become insoluble. Insoluble tau self-aggregates and yields NFTs, which compromises tau's cytosolic functions, dysregulating intracellular homeostatic mechanisms and leading to neuronal death (Mudher & Lovestone, 2002).

Furthermore, A β -mediated neurotoxicity has been shown to require tau. Cognitive decline associated with A β aggregation occurs only when accompanied by elevated levels of PHF-tau, which suggests that A β is an upstream modulator of tau hyperphosphorylation (Peric & Annaert, 2015).

2.1.3 Inflammation

Inflammation is an immune response in which affected tissue responds to harmful stimuli. Inflammatory mediators help increase blood flow and accumulate defense cells in affected areas (Institute for Quality and Efficiency in Health Care, 2015). Microglia are brain immune cells that act similarly to macrophages in recognizing A β plaques as a signal of brain tissue damage (Mandrekar & Landreth, 2010). Once microglia are activated, they produce chemokines, a type of pro-inflammatory signaling protein, to signal for more microglia activity to respond to the toxic A β plaque signal (Yoon & Kim, 2015).

Although microglia are necessary in maintaining homeostasis under normal physiological conditions, long-term microglial activation can have detrimental effects on neurons. In the presence of a manageable amount of A β plaques, microglia can successfully clear these plaques through phagocytosis and without a large inflammatory response (Mandrekar & Landreth, 2010). However, once plaque development reaches more severe pathological levels, the phagocytic capabilities of

microglia plateau. Although the A β plaques can be internalized, digestion of these dense plaques is difficult within the phagocytic microglia (Yoon & Kim, 2015; Mandrekar & Landreth, 2010). Thus, not all phagocytic activity completes A β plaque digestion, which can lead to a cascade of microglial aggregates surrounding tissue regions with high plaque content. This initiates a positive inflammatory feedback loop because microglia recruited to digest the plaques fail and begin to send distress signals, attracting even more microglia. Microglia release chemokines to create a pro-inflammatory environment in the brain. This reduces the phagocytic capabilities of microglial cells and causes further A β aggregation (Mandrekar & Landreth, 2010).

2.1.4 Apoptosis

Another major hallmark of AD is brain atrophy due to elevated levels of apoptosis triggered by the pathological A β plaques and NFTs (Xu et al., 2012). While this programmed cell death process is important for removing damaged or unnecessary cells, elevated levels deplete healthy brain cells that are important for proper functioning. Apoptosis has two operating pathways, both of which are relevant to AD: extrinsic, which is activated by cell-surface death receptors, and intrinsic, which involves signals from mitochondria (Xu et al., 2012).

In an extrinsic pathway (Figure 2), a signaling molecule called a Fas ligand attaches to a Fas death receptor on the surface of the cell, triggering the formation of a death-inducing signaling complex (DISC) in response to external apoptotic signals, such as A β plaques. Effector caspases induce apoptosis through a caspase cascade triggered by initiator caspases within the DISC. Initiator caspases, such as caspase 8, activate effector caspases that then follow a cascade to activate caspases 3, 6, and

7. Executioner caspases such as these activate target proteins that break down the cell from the inside (Figure 2; Andersen, Becker & Straten, 2005).

The intrinsic apoptosis pathway is mediated by mitochondria and initiated by the presence of cytoplasmic cytochrome c, which is suggestive of mitochondrial dysfunction and oxidative stress. Mitochondria regulate both energy metabolism and cell death pathways, fulfilling the high-energy requirements of the brain and stimulating apoptosis when necessary. Therefore, mitochondria are appropriate indicators of neuron survival (Moreira et al., 2012). This link between apoptosis and mitochondrial dysfunction corresponds with the increased risk that age contributes to AD. Oxidative stress also causes mitochondria to become larger and more disorganized, especially with age. This oxidative stress and mitochondrial dysfunction relates to AD beyond the apoptosis that occurs in the disease. It also relates to AD through aberrations in glucose metabolism that yield oxidative stress because cells are not getting necessary amounts of glucose. The presence of cytoplasmic cytochrome c is analogous to the caspase 8 signal in the extrinsic apoptosis pathway. Cytochrome c triggers formation of an apoptosome, which is followed by caspase 3, 6, and 7 activation that goes on to degrade the cell (Figure 2).

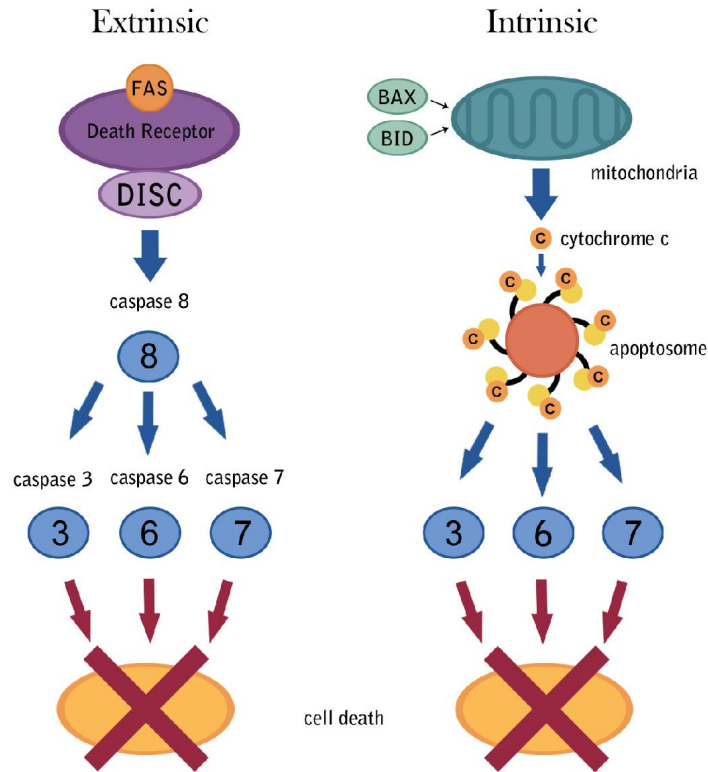


Figure 2. Apoptosis Signaling Pathway. In the extrinsic pathway on the left, a Fas ligand attaches to a Fas death receptor and triggers formation of a DISC. The initiator caspase 8 activates effector caspases 3, 6, and 7 through a cascade, which causes cell death. In this intrinsic pathway, mitochondria and cytochrome c can trigger apoptosis through formation of an apoptosome that activates caspases 3, 6, and 7. This causes cell death. Information from Alberts et al., (2008). Created by A. Zachery.

Studies on apoptotic processes in AD have highlighted an important link between the intrinsic apoptotic pathway and improper APP proteolysis. As previously discussed, APP is normally broken down by α - and γ -secretases to produce sAPP α , which, among other functions, serves as a protective factor for neurons

against apoptosis (Zhang, Ma, Zhang & Xu, 2012). In AD, apoptosis is triggered by alternative cleavage of APP by β -secretase rather than α - and γ -secretases. This activates caspases 3 and 7 to trigger cell death (Fiorelli, Kirouac & Padmanabhan, 2013). In addition to starting this self-destruct mechanism, the improper cleavage of APP results in aggregated $A\beta$ proteins, which inhibits production of protective sAPP α (Figure 3). A decreased amount of sAPP α may contribute to brain degeneration in AD subjects (Zhang, Ma, Zhang & Xu, 2012). For these reasons, caspase inhibitors are being studied as a potential therapy for AD.

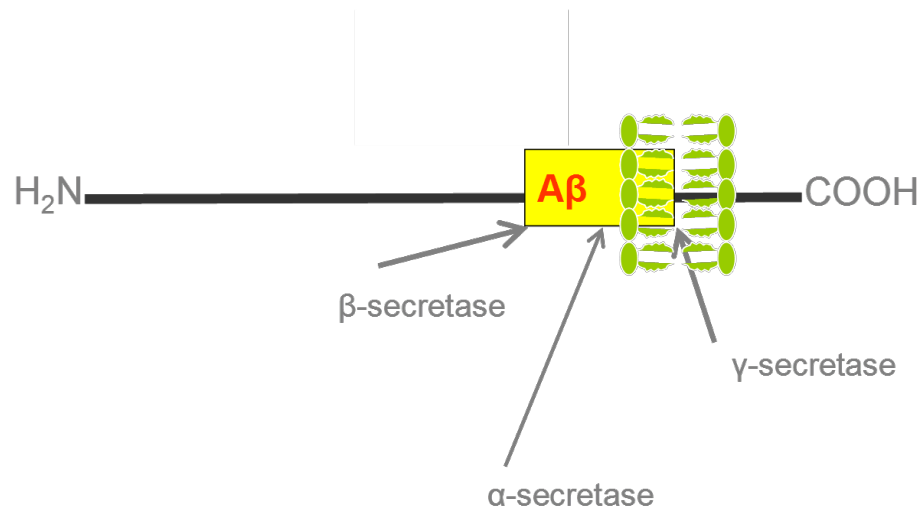


Figure 3. APP Processing. β -secretase cleavage of the N-terminal fragment of APP followed by action of γ -secretase in the membrane releases $A\beta$ and leads to accumulation of the $A\beta_{1-40}$ and $A\beta_{1-42}$ peptides. Used with permission from Dr. Kara Duffy (2012).

2.1.5 Diminished Cerebral Glucose Metabolism

Diminished cerebral glucose metabolism (DCGM), or glucose hypometabolism, characterizes the abnormality in glucose metabolism occurring in AD (Small et al., 2000). Studies ubiquitously show that severity of AD is highly correlated with glucose hypometabolism (Mosconi, Pupi & De Leon, 2008). This problem with glucose metabolism is a reason that AD is referred to as “Type III Diabetes” (Sebastiao et al., 2014). Glucose metabolism levels can be measured using PET scanning, which tracks disease progression (Levy, Zieve, & Ogilvie, 2014). When glucose metabolic levels were tracked in subjects with the APOE- ϵ 4 genetic risk factor for sporadic AD, DCGM was found before detectable AD symptoms could be observed (Small et al., 2000). Another study expanded on this study and showed that the incidence of DCGM in these APOE- ϵ 4 carries often occurs decades before other detectable AD symptoms, at a mean age of 30.7 years, long before any cognitive impairment (Reiman & Chen et al., 2004).

It remains unclear if glucose hypometabolism is a cause of AD or a symptom of AD. In AD’s earliest stages, glucose hypometabolism begins in the hippocampus and later spreads throughout nearly all cortical areas (Santi et al., 2001). One probable explanation of DCGM preceding AD onset is that deficient energy metabolism would change the oxidative environment of neurons. This contributes to the progression of AD, resulting in a positive feedback mechanism of mitochondrial dysfunction and disrupted glucose metabolism (Mosconi et al., 2008).

2.2 Glucose Metabolism

As discussed above, DCGM is an important aspect of AD pathology. DCGM research is a promising field of AD research, especially given the newly found relationship between AD and T2D. A comprehensive understanding of DCGM requires a discussion of glucose uptake and metabolism.

The body's main source of energy is adenosine triphosphate (ATP), which is generated primarily through the oxidative metabolism of glucose. Peripheral glucose levels are modulated by the pancreas; when blood sugar is low, the pancreas secretes glucagon. Glucagon then signals the liver to break down stored glycogen into glucose, and the glucose is released into the bloodstream to return blood sugar to homeostatic levels (Leibiger, Leibiger & Berrgren, 2008). When blood sugar is high the pancreas secretes insulin, which transports glucose into cells and lowers blood sugar. This facilitation of glucose into peripheral cells is regulated by the ISP. In this pathway, extracellular insulin initiates an intracellular cascade of proteins that eventually activates glucose transporter 4 (GLUT4) to allow glucose into the cell (Leibiger, Leibiger & Berrgren, 2008).

In the body's periphery, GLUT4 and insulin are the main regulators of glucose uptake (Huang & Czech, 2007). The brain and CNS mainly depend on insulin-independent mechanisms for glucose uptake, but insulin and GLUT4 still regulate some aspects of glucose metabolism in the brain (Bingham et al., 2002). The differences between glucose metabolism in the body and the brain necessitates an analysis of glucose metabolism in the CNS.

2.2.1 Glucose Metabolism in the Brain

Glucose is the fundamental source of energy in the brain, and the brain exhausts approximately 60% of the body's available glucose in its resting state (Berg, Tymoczko & Stryer, 2002; Mobbs, Kow & Yang, 2001). The brain consumes 120 grams of glucose per day, primarily to maintain ion concentration gradients. These gradients are responsible for both the transmission of electrical information and neurotransmitter synthesis (Berg et al., 2002). Due to the brain's high metabolic demand, glucose must be facilitated across the BBB at a consistently high rate, regardless of fluctuations of blood glucose concentration or insulin levels. For this reason, insulin-dependent GLUT4 is not the main glucose transport mechanism in the brain. Instead, insulin-independent glucose transporter 1 (GLUT1) and glucose transporter 3 (GLUT3) transporters are the major mechanisms by which glucose enters the CNS (El Messari et al., 2002).

Glucose must be transported from the bloodstream through both the BBB and neuronal membranes in order to be metabolized in neurons (Figure 4). GLUT1 is mainly responsible for the constitutive transport of glucose through the BBB and GLUT3 is mainly responsible for the transport into neurons (Klepper & Voit, 2002; Simpson et al., 2008). GLUT3 has a strong affinity for binding glucose, so even low glucose levels do not deter the rate of glucose uptake (Schulingkamp, Pagano, Hung & Raffa, 2000). This feature of GLUT3 helps to satiate the brain's high metabolic demand.

Since the majority of glucose metabolism in the brain is insulin independent, researchers did not have reason to believe GLUT4 is present and its discovery

occurred only recently. The presence of GLUT4 and insulin receptors in the brain has now been experimentally proven (Shah, DeSilva & Abbruscato, 2012).

Similarly to glucose, insulin is not produced in the brain and cannot passively diffuse through the BBB; it requires controlled receptor-mediated transport (Sartorius et al., 2015). These transporters are expressed at various locations in the BBB but are most abundant in the olfactory bulb (Banks, Owen & Erickson, 2012). Additionally, insulin receptors (IRs) are expressed throughout the cortex and hippocampus, allowing for insulin entry into neurons (Woods, Seeley, Baskin & Schwartz, 2003). IRs are generally more prevalent in areas with high GLUT4 concentrations, especially in motor areas and the hippocampus (Choeiri, Staines & Messier, 2002; El Messari et al., 2002). Although the metabolic demand of the brain restricts insulin from completely controlling glucose uptake, insulin does act as a modulator to alter glucose uptake in some brain regions (Willette et al., 2015). The hippocampus and subiculum in particular express high levels of GLUT4 messenger ribonucleic acid (mRNA). The hippocampus is also associated with learning, memory, and AD pathology. Additionally, A β plaque formation begins in the subiculum, which is why the presence of GLUT4 in the hippocampus and subiculum is important to the present study (George et al., 2014). Understanding and researching the different aspects of glucose metabolism is imperative to the study of AD, as AD relates to DCGM characterized by faulty glucose metabolism.

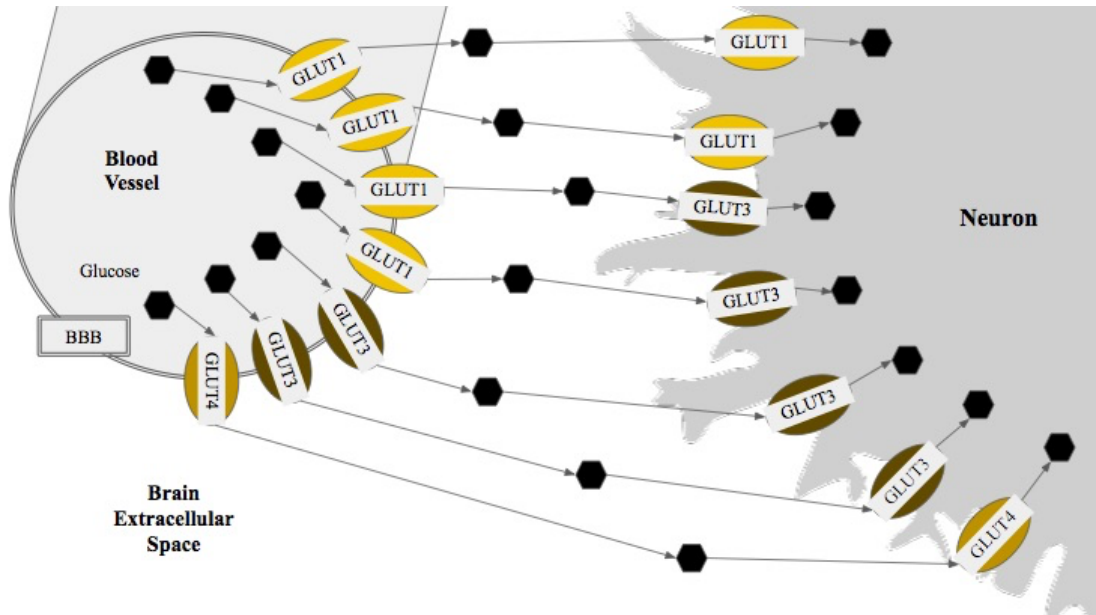


Figure 4. Glucose Transport in the CNS. *Glucose is transported from the bloodstream across the BBB to the brain extracellular space. In the BBB, the most abundant glucose transporter is GLUT1, although GLUT3 and GLUT4 are also expressed in lower quantities. From the brain extracellular space, glucose enters neurons through more glucose transporters. In the neurons, the most abundant glucose transporter is GLUT3, although GLUT1 and GLUT4 are also expressed.*
 Information from: Shah, DeSilva, & Abbruscato, 2012. Created by S. Morken.

2.3 Insulin Signaling Pathway

The relationship between AD and T2D suggests that the insulin-dependent mechanisms of glucose uptake may contribute to AD and DCGM. Therefore, this research focuses on how insulin signaling affects AD and requires a background on the ISP and its components (Figure 5).

The Phosphoinositide 3-kinase (PI₃K) pathway of insulin signaling is the cell transduction mechanism primarily responsible for translocation of GLUT4 to the plasma membrane (Yin et al., 2006; Chang, Chiang & Saltiel, 2004). Extracellular insulin initiates an intracellular signal cascade that eventually translocates GLUT4 (Yin et al., 2006). In the PI₃K pathway, insulin binds to the IR, which activates signaling protein Insulin Receptor Substrate 1 (IRS1) by tyrosine kinase phosphorylation (Yin et al., 2006). IRS1 is the link between insulin receptor stimulation and the downstream ISP mechanisms that lead to transcription and reprogramming of cells (De Felice et al., 2014). Activated IRS1 binds to the P85 subunit of the PI₃K molecule, which then activates Phosphoinositide dependent protein kinase-1 (PDK1), a master kinase that activates isoforms of protein kinase B (Akt1 and Akt2), and protein kinase C zeta (PKC ζ) (Yin et al., 2006).

Akt1 is a protein kinase that inhibits apoptosis and induces protein synthetic pathways to promote tissue growth (Kupriyanova & Kandror, 1999). Akt2 not only prevents apoptosis but also ultimately leads to translocation of GLUT4 to the plasma membrane (Kupriyanova & Kandror, 1999). PDK1 also phosphorylates and activates PKC ζ , which associates with GLUT4 and aids in its translocation to the plasma membrane (Braiman et al., 2001).

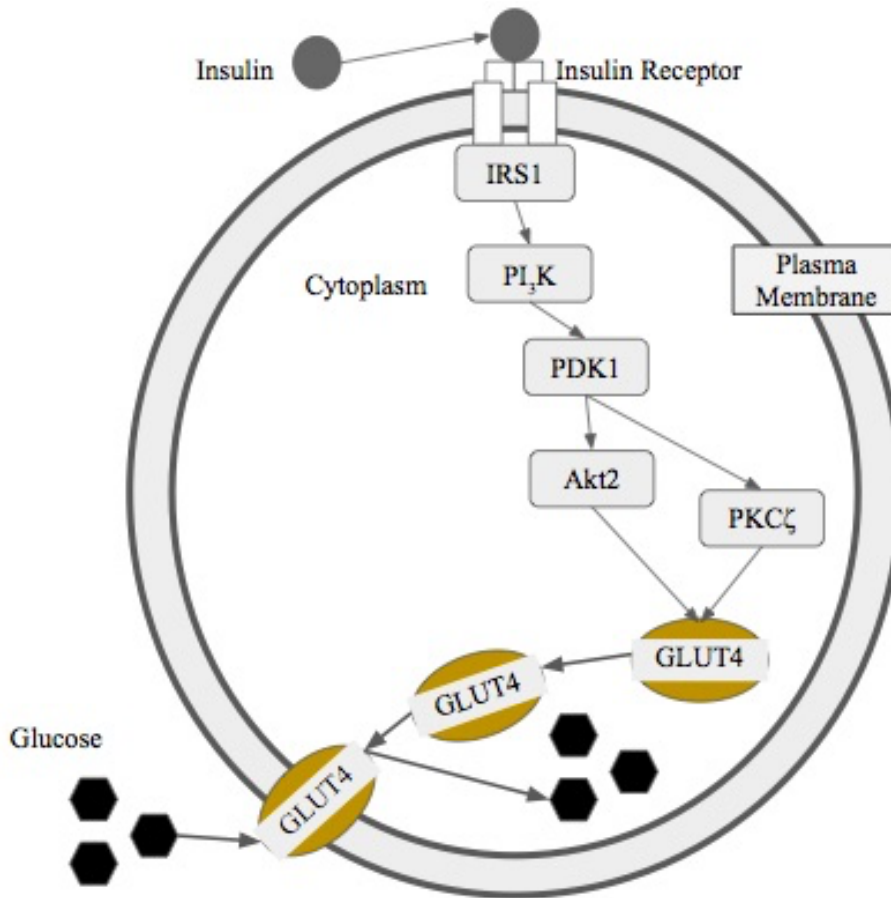


Figure 5. Simplified ISP. *Insulin binds to the insulin receptor and stimulates a cascade, ultimately resulting in the translocation of GLUT4 transporters.* Information from: Braiman et al. 2001; Kupriyanova & Kandror, 1999; Yin et al., 2006. Created by S. Morken.

This translocation can also be triggered by the activation of a Cbl/Cbl-associated protein (CAP) complex. Insulin can directly stimulate the activation of Cbl/CAP (Monsalve, Pyarasani, Delgado-Lopez & Moore-Carrasco, 2013). When bound by insulin, Cbl, a receptor adapter protein, is recruited to the IR by CAP (Leto & Saltiel, 2012). This performs a similar function to PI₃K and facilitates the translocation of GLUT4 to the plasma membrane (Leto & Saltiel, 2012).

2.3.1 PPAR γ

A focus of this study is the role of the nuclear receptor (NR) Peroxisome Proliferator-Activated Receptor gamma (PPAR γ). Two relevant NRs, or transcription factors, within the ISP are retinoid X receptors (RXRs) and PPARs (Leonardini, Laviola, Perrini, Natalicchio & Giorgino, 2009). PPAR γ is a common isoform of PPAR that is involved in many bodily processes including lipid storage, energy metabolism, adipocyte differentiation, inflammation, and insulin sensitivity (Mandrekar-Colucci, Karlos & Landreth, 2012; Mandrekar-Colucci & Landreth, 2011).

PPAR γ is a component of the downstream ISP that aids in increasing glucose uptake using two major strategies: transcription and translocation (Figure 6). PPAR γ facilitates the transcription of adiponectin, GLUT4, and Cbl/CAP (Figure 7). PPAR γ 's insulin-dependent activation begins with the heterodimerization of PPAR γ and RXR to create a transcription factor complex associated with a corepressor (Mandrekar-Colucci et al., 2012). This dimer is bound to the PPAR response element (PPRE), which is located near the promoter of the target gene (Mandrekar-Colucci et al., 2012; Leonardini et al., 2009). When no ligand is present, the promoter is in a repressed state that prevents transcription and represses the NRs, blocking gene expression. Upon ligand binding, conformational change of the dimer induces corepressor release and coactivator association, releasing the complex from the PPRE and allowing for transcriptional proteins to bind to the PPRE. This yields gene transcription of adiponectin, GLUT4, and Cbl/CAP (Mandrekar-Colucci et al., 2012). The transcription of GLUT4 and adiponectin help provide more pathways for

glucose to enter the cell and improve insulin sensitivity (Monsalve et al., 2013). Transcription of the Cbl/CAP complex enhances its translocating function of cytosolic and newly transcribed GLUT4 (Chiang et al., 2001). It is for these reasons that PPAR γ is considered an insulin sensitizer.

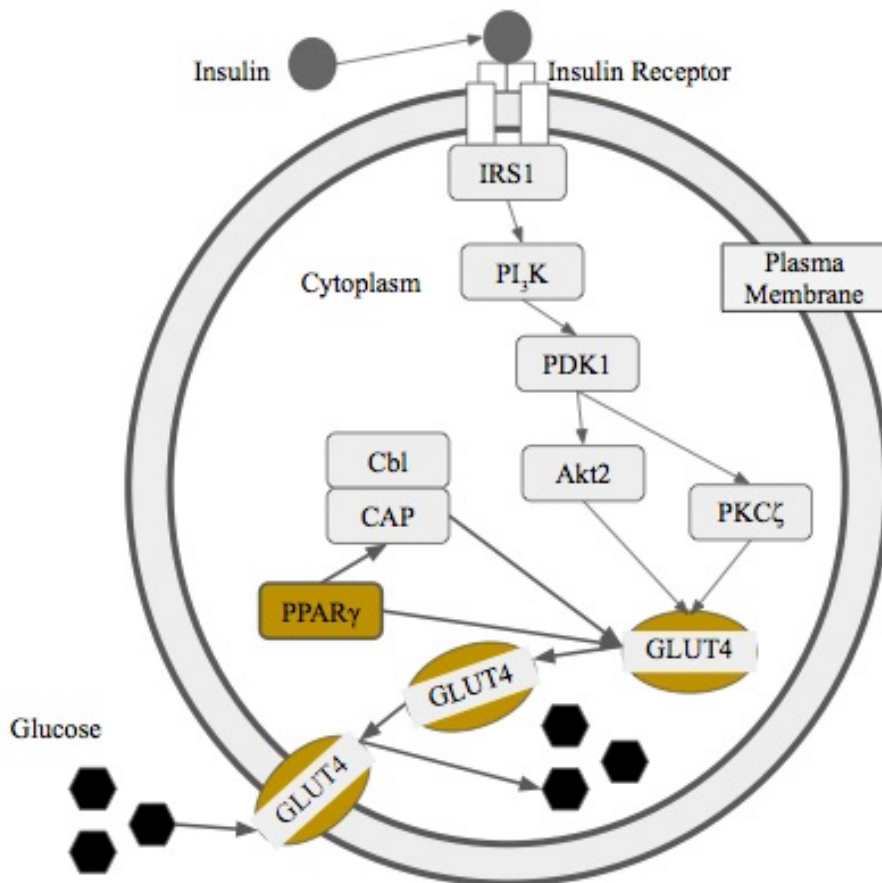


Figure 6. Simplified ISP Including PPAR γ . PPAR γ stimulates GLUT4 directly and through the Cbl/CAP complex. Information from: Braiman et al., 2001; Kupriyanova & Kandror, 1999; Leonardini, Laviola, Perrini, Natalicchio & Giorgino, 2009; Leto & Saltiel, 2012; Monsalve, Pyarasani, Delgado-Lopez & Moore-Carrasco, 2013; Yin et al., 2006. Created by S. Morken.

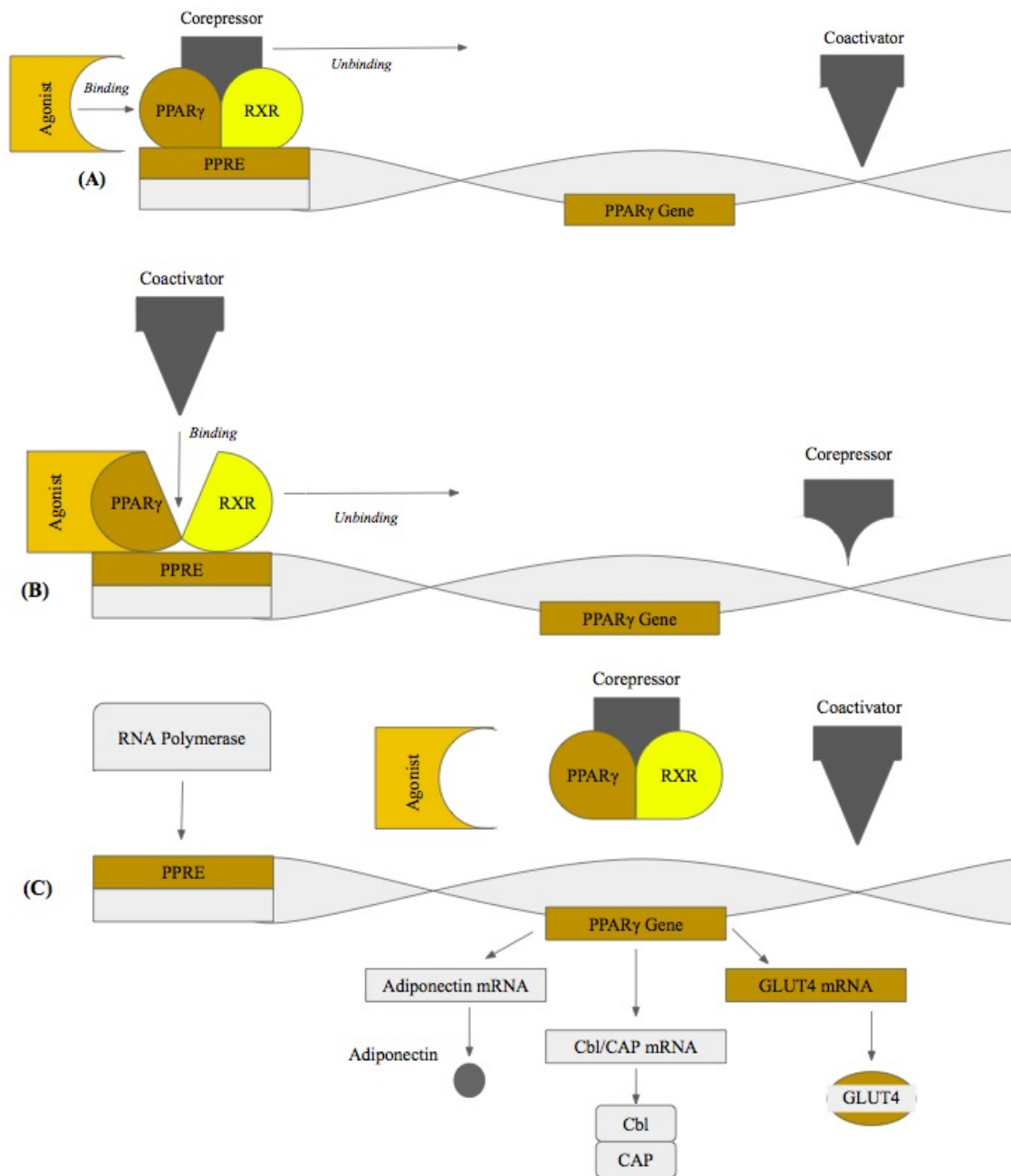


Figure 7. The Insulin-dependent Mechanism of PPAR γ Gene Transcription. (A) In the unstimulated state, PPAR γ and RXR heterodimerize and associate with a corepressor. This complex is bound to the PPRE, blocking gene expression. When an agonist binds to PPAR γ , conformational changes cause the corepressor to fall off the complex. (B) Next, a coactivator associates with the complex. This causes another

conformational change, which forces the complex off of the PPRE. (C) The absence of any complex on the PPRE allows transcriptional proteins like RNA polymerase to bind. RNA polymerase transcribes the gene to an mRNA that can get translated into proteins like adiponectin, Cbl/CAP, or GLUT4. Information from: Mandrekar-Colucci et al., 2012; Leonardini et al., 2009; Monsalve et al., 2013; Chiang et al., 2001. Created by S. Morken.

Beyond its role in the ISP, PPAR γ is also an anti-inflammatory compound. In addition to its expression in metabolic tissue, PPAR γ is expressed in a variety of immune cells (Széles, Töröcsik & Nagy, 2007). Expression of PPAR γ in immune cells inhibits inflammatory responses through its NR activity by decreasing macrophage activity (Széles et al., 2007).

Understanding the activation of PPAR γ is a key component to this study. PPAR γ agonists are insulin sensitizers and allow more glucose to enter the cell. This insulin-dependent mechanism of PPAR γ and its effect on AD will be studied, as well as the anti-inflammatory aspects of PPAR γ that affect other components of AD pathology.

2.4 Current Alzheimer's Disease Research: Thiazolidinediones and Insulin

Current AD research focuses on treating the glucose hypometabolism using both insulin and PPAR γ agonists. One PPAR γ agonist currently being studied in relation to AD is TZD (Stratchen, 2005).

2.4.1 Thiazolidinediones and Alzheimer's Disease

PPAR γ agonists such as TZDs help alleviate some symptoms and pathologies of AD. PPAR γ agonists have been found to improve learning in AD patients and reduce amyloid burden and plaque load in animal models (Liu, Wang, & Jia, 2015). Through PPAR γ activation, TZDs both administered orally and directly-injected have been shown to reduce the different forms of AD pathology in multiple AD mouse models, including the triple-transgenic model (3x-Tg-AD) used in this study (Tamez-Pérez, Quintanilla-Flores, Rodríguez-Gutiérrez, González-González & Tamez-Peña, 2015). Two common types of TZDs are Rosiglitazone (RGZ) and PGZ (Gupta & Gupta, 2012).

Through PPAR γ activation, TZDs have been shown to delay AD development using a variety of mechanisms affecting multiple AD pathologies (Zolezzi & Inestrosa, 2013). TZDs have been shown to reestablish insulin sensitivity, reduce inflammation, clear A β plaques, increase mitochondria function, and prevent tau hyperphosphorylation (Winkelmayer, Setoguchi, Levin & Solomon, 2008; Lee, Hsu, Liao & Pan, 2011; Mandrekar-Colucci & Landreth, 2011; Tamez-Pérez et al., 2015).

PPAR γ increases the number of GLUT4 transporters in neuronal membranes, allowing increased glucose uptake and facilitating proper cellular function. TZD activates PPAR γ and Akt2 to stimulate glucose uptake into cells. This also indirectly stimulates GLUT4 translocation by activating the Cbl/CAP complex (Leonardini, Laviola, Perrini, Natalicchio & Giorgino, 2009). In addition, TZD protects against inhibitory phosphorylation of IRS1 to increase insulin sensitivity (Lee, Hsu, Liao &

Pan, 2011). Therefore, TZDs increase glucose uptake through upregulation of GLUT4 (Figure 8). This combats the AD brain's decreased sensitivity to insulin.

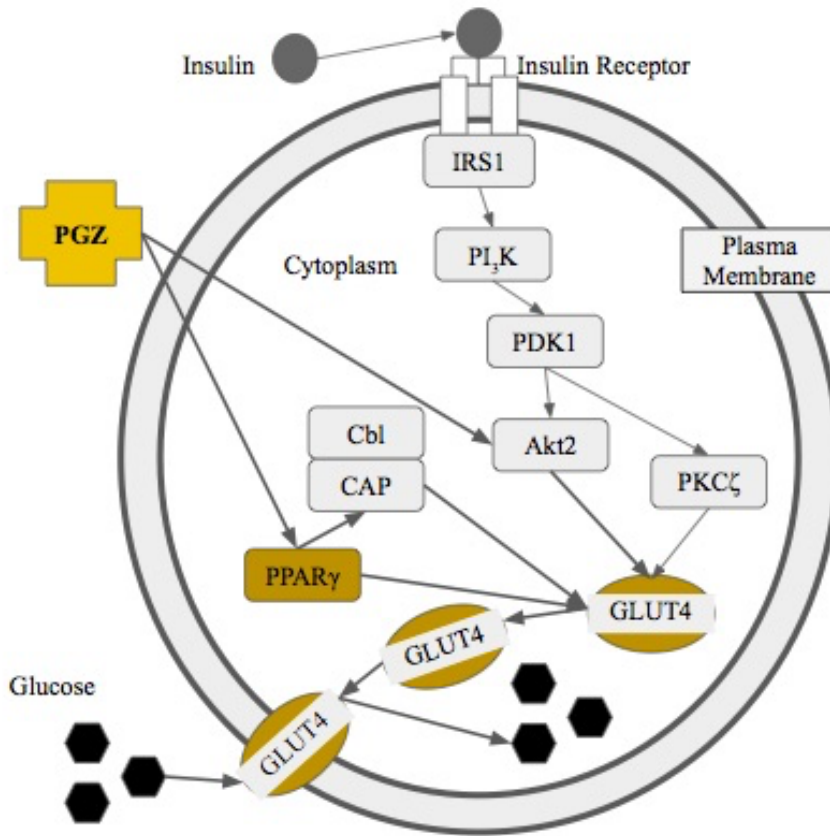


Figure 8. Simplified ISP Including PPAR γ and PGZ. PGZ stimulates both PPAR γ and AKt2 to increase glucose uptake in cells through GLUT4 translocation.

Information from: Braiman et al., 2001; Kupriyanova & Kandror, 1999; Leonardini, Laviola, Perrini, Natalicchio & Giorgino, 2009; Leto & Saltiel, 2012; Monsalve, Pyarasani, Delgado-Lopez & Moore-Carrasco, 2013; Yin et al., 2006. Created by S. Morken.

Additionally, PPAR γ agonists reduce inflammation by polarizing microglia to the anti-inflammatory (M2) state. This occurs through gene transactivation and gene suppression (Mandrekar-Colucci & Landreth, 2011). When the inflammatory response of macrophages is triggered by A β plaques, the increased levels of microglia and macrophages become neurotoxic and damage the brain. Macrophages produce interleukin-6 (IL-6), which activates more macrophages, inflammatory agents, and tumor necrosis factor alpha (TNF α), which induces apoptosis (Rubio-Perez & Morillas-Ruiz, 2012; Tamez-Pérez et al., 2015). PPAR γ activated by TZD acts as anti-inflammatory agent by stopping the transcription of the nuclear factor Activator Protein 1 (AP-1). This prevents microglia from becoming activated by A β plaques.

Another function of TZD is the clearance of A β plaques. The high AD risk allele, ApoE- ϵ 4, is associated with reduced A β plaque clearance (Perez & Quintanilla, 2015). TZDs overexpress ApoE and increase A β clearance (Tamez-Pérez et al., 2015). There is also research showing that treatment with TZDs reduces the expression of the beta-secretase 1 (BACE1) enzyme that improperly cleaves APP in AD (Liu, Wang, Yan, Zhang, Pang & Liao, 2013).

TZDs also prevent tau hyperphosphorylation in the hippocampi of both T2D and 3x-Tg-AD mouse models. In AD, cyclin-dependent kinase 5 (Cdk5), which phosphorylates APP and tau, is overactive and phosphorylates both of these proteins at a faster rate than dephosphorylation. This results in A β plaques and NFT protein aggregates (Liu et al., 2015). PPAR γ decreases the levels of p35, a Cdk5 activator, which prevents Cdk5 from hyperphosphorylating tau. PPAR γ also downregulates the

c-Jun N-terminal kinase (JNK) signaling pathways in which Cdk5 is involved (Tamez-Pérez et al., 2015).

Finally, TZDs increase mitochondria function. Mitochondria in neurons are damaged from oxidative stress in AD. A study of A β -injected Wistar rats, a model used to study aging, found that long-term TZD treatment reduced oxidative damage and produced more mitochondria. Long-term potentiation (LTP), an important part of synaptic plasticity, was also increased with TZD treatment (Tamez-Pérez et al., 2015; Prakash & Kumar, 2014).

2.4.2 Insulin and Alzheimer's Disease

Some research suggests that the hyperinsulinemia associated with T2D is a risk factor for developing AD because it leads to decreased insulin signaling in the brain. Decreased insulin signaling reduces the inhibition of a major tau kinase, thereby preventing phosphorylation of tau (Chami et al., 2016).

Two important proteins in AD are JNK and TNF α . Increased JNK and TNF α activity has been recorded in transgenic AD mice models, monkeys injected with A β oligomers, and post-mortem brains from AD patients (De Felice et al., 2014). In T2D, TNF α stimulation induces apoptosis and inhibits IRS1 by phosphorylation (Tamez-Pérez et al., 2015; De Felice, Lourenco & Ferreira, 2014). This phosphorylation causes cells to become insulin resistant by blocking the downstream mechanisms of the ISP and causing the insulin receptors on the cell membrane to internalize (De Felice et al., 2014). TNF α also triggers a JNK stress pathway that inhibits IRS1 by phosphorylation (De Felice et al., 2014).

A β peptides decrease insulin's affinity for its receptor. They are also competitive insulin inhibitors through the function of insulin degrading enzyme (IDE), which acts on both insulin and A β peptides (Farris et al., 2003). The ApoE- ϵ 4 gene has been associated with decreased levels of IDE (Wang, Dickson & Malter, 2006). This gene also reduces IDE levels by activating N-methyl-D-aspartate (NMDA) receptors in hippocampal neurons. IDE will degrade A β proteins in the absence of high levels of insulin. However, if insulin is able to bind to the IRs, insulin levels will increase, which in turn will cause an increase in IDE that can degrade more A β plaques (Du, Chang, Guo, Zhang & Wang, 2009).

2.4.3 Intranasal Administration of Insulin and Thiazolidinediones

Many current insulin studies administered treatment intranasally to focus doses in the CNS and cross the BBB. For a molecule to cross the BBB, three main criteria are considered: hydrophilicity versus lipophilicity, molecular weight, and degree of ionization. Molecules that are lipophilic, nonionized, and have a molecular weight of less than 300 Daltons yield the quickest and most efficient absorption (Grassin-Delye et al., 2012).

During intranasal administration, treatments enter the nasal cavity and are then absorbed by the nasal mucosa through passive diffusion. Molecules then enter the brain either through axonal transport or by bulk flow through the olfactory and perineural channels of the extraneuronal pathway (Talegaonkar & Mishra, 2004; Hanson, Fine, Svitak & Faltsek, 2013).

One study investigated the effects of eight weeks of intranasal insulin administration on declarative memory, attention, and mood in healthy human subjects

(Benedict et al., 2004). Results showed that subjects experienced improvement in recall of words and enhanced mood. Blood glucose and plasma insulin remained constant between treatment and placebo groups, which indicated that the intranasal method did not cause peripheral side effects.

Another study tested the effect of intranasal insulin administration on both cognition and A β peptides. Intranasal insulin treatment was administered daily to patients with early AD for 21 days (Reger et al., 2007). Like the previous study, plasma glucose and insulin levels were unchanged between the treatment and placebo groups. The insulin-treated subjects retained more verbal information and showed improved attention when compared to the placebo-assigned subjects (Reger et al., 2007).

Although intranasal insulin has been studied extensively, TZDs have never been administered intranasally (Freiherr et al., 2013). Intranasal administration of insulin for researching and treating AD provides a framework for this research method. Combining the method of intranasal administration with PGZ, an insulin sensitizer, allows examination of the role of the ISP and T2D drugs in AD development and pathology. Additionally, the aforementioned studies have indicated that intranasal insulin administration does not have systemic effects (Benedict et al., 2004). Based on this, it can be predicted that intranasal PGZ administration would impact only the CNS.

Chapter 3: Research Strategy

The purpose of the study was to further elucidate the role of the downstream ISP in the development of AD pathology. PGZ was chosen as the type of TZD investigated in this study as it has fewer side effects, especially negative cardiovascular effects, than RGZ does (Winkelmayer, Setoguchi, Levin & Solomon, 2008). PGZ and insulin were administered intranasally in order to address the following research questions:

1. Does intranasal administration of PGZ and insulin sensitize IR signaling to increase glucose metabolism?
2. Will three weeks of PGZ and insulin treatment reduce AD pathology?
3. Do reductions in pathology persist two weeks after completing the dosing regimen?

The combined treatment of insulin and PGZ was hypothesized to create longer lasting effects and reduced AD pathology in comparison to an insulin only treatment as a result of improved glucose uptake. An initial pilot study was performed on non-transgenic mice in order to validate and refine methods of intranasal administration of PGZ and insulin. The main study was then performed on an AD mouse model, and was carried out in three phases to address the research questions.

3.1 Intranasal Method

The intranasal method was used to administer treatments in this study because it is clinically safe, and targets delivery to the CNS while reducing unwanted

peripheral effects in the blood (Talegaonkar & Mishra, 2004). A safety study of intranasally administered insulin revealed no nasal irritation or differences in blood glucose concentrations (Kupila et al., 2003).

As previously noted, PGZ does not easily cross the BBB through the bloodstream (Maeshiba et al., 1997). Therefore, an intranasal method of delivering PGZ was developed in this study in order to bypass the BBB and enter the brain through the olfactory pathway, mirroring intranasal insulin administration.

3.2 Pilot Study

In order to refine the intranasal delivery method, a pilot study was performed in order to determine if intranasal administration of PGZ was viable and to determine an optimal dose of intranasal PGZ, as there was no precedent from previous literature. Glucose uptake was measured through fluxomics analysis in order to assess the effects of PGZ administration and its ability to pass the BBB.

Additionally, the pilot study supported aims of the Institutional Animal Care and Use Committee (IACUC) to reduce the number of and risk to animals used for the Main Study. Thus, both technique and feasibility were affirmed and refined with the Pilot Study.

Previously, studies using PGZ only involved oral administration of the drug. The dosage of intranasal PGZ was determined by referring to the dose of oral PGZ given in previous studies for peripheral metabolism (Heneka et al., 2005). Then, the weight and metabolism rate of the brain was used to calculate an intranasal dose. These calculations yielded 30.6 μg of PGZ per intranasal administration.

Based on this calculation, three dosing amounts were tested – 15 µg, 30 µg, and 60 µg. Each PGZ concentration was combined with 120 µg of insulin dissolved in a 24 µL dose (Renner et al., 2012). A detailed record of the calculations can be found in Appendix D.

Eight nontransgenic C57/BL6 mice, which demonstrated no AD pathology, were assigned to four experimental groups. Two mice received intranasal administration vehicle only (acidic saline) as a control. Additional groups of mice received 15 µg of PGZ (n = 2), 30 µg of PGZ (n = 2), and 60 µg of PGZ (n = 2) each dissolved in 24 µL of acidic saline. Treatments were administered, behavioral responses were noted, and mice were given an intraperitoneal injection of ¹³C-labeled glucose tracer. Mice were necropsied for sample collection 24 hours after drug administration, and brains were extracted for fluxomics analysis. Results obtained from the fluxomics analysis indicated all doses of PGZ increased brain glucose uptake when compared to the control, and the largest increase occurred with 60 µg PGZ. Based on these results, 60 µg was selected as the optimal dose of PGZ for the Main Study.

3.3 Experimental Design: Main Study

3.3.1 Mouse Model

The majority of AD research is conducted using transgenic rodent models expressing familial gene mutations. Mouse models are appropriate for research on both familial and sporadic AD because both of these subtypes share similar clinical and post-mortem characteristics (Chin, 2011).

A 3x-Tg-AD mouse model was used in this study, which contained the PS1_{M146V}, tau_{P301L}, and APP_{Swe} transgenes (Oddo et al., 2003). The addition of human APP and tau transgenes causes the mouse model to exhibit both plaques and tangles, serving as an appropriate model to study AD (Chin, 2011). In the 3x-Tg-AD model, there is no meaningful difference in pathology between male and female mice, so both sexes were used in the study (Oddo et al., 2003). Expected pathological onset of this mouse strain, defined by when significant amounts of both A β plaques and tau tangles would be detectable, was anticipated to occur at 12-15 months of age (Blázquez, Cañete, Tobeña, Giménez-Llort & Fernández-Teruel, 2014).

The 3x-Tg-AD mouse has been an effective model to study the effects of insulin on AD pathology. Vandal et al. (2014) investigated the effects of a single insulin dose on the increased memory impairments caused by a high-fat diet in a 3x-Tg-AD mouse model. The insulin dose reduced the memory effects and A β levels and not only did the model effectively mimic desired AD pathology, but the experiment further supports the link between AD and T2D. Another study by Sancheti et al. (2014) used a younger 3x-Tg-AD mouse model to investigate the therapeutic effects of lipoic acid, a compound that mimics insulin, on the hypermetabolism associated with AD. Glucose metabolism was measured with a similar ¹³C labeling method to the proposed study, and the lipoic acid was found to reduce hypermetabolism in the model to levels of a control model. Searcy et al. (2012) used the 3x-Tg-AD mouse model to investigate the effects of oral pioglitazone on AD pathology and confirmed the results of prior animal studies that TZDs can have a therapeutic effect on AD pathology by ameliorating cognitive deficits.

The literature has demonstrated that this mouse model not only develops similar AD pathology to humans, but it also responds to treatment with insulin and TZD accordingly, making it a reasonable model to use for the proposed study.

3.3.2 Subiculum

The subiculum is a subregion of the hippocampus (Figure 9) where plaque formation begins (George et al., 2014). Because many relevant AD pathological markers are present in this region, the subiculum was identified as the area of interest when analyzing immunohistochemistry (IHC) results. In addition, unpublished pathological progress data suggests that the subiculum is an appropriate structure to use for analysis of IHC endpoints, specifically in the colony of 3x-Tg-AD mice used for this study (unpublished data, Ottinger Lab).

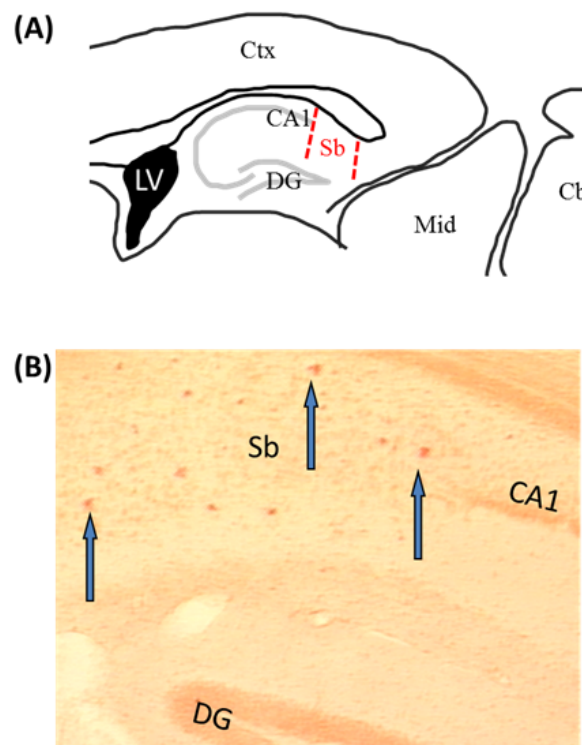


Figure 9. Anatomical Features of a Mouse Brain. (A) Schematic Representation of Sagittal View of Mouse Brain Displaying Anatomical Features and their Spatial

Relationships. Modified from Paxinos and Franklin (2001). (B*) Congo red staining was utilized to visualize amyloid plaque formation in 14-month old 3x-TTG, arrows denote selected plaques. LV = lateral ventricle, CA1 = CA1 Hippocampus, DG = dentate gyrus, Ctx=Cortex, Mid = Midbrain, Cb=Cerebellum. * Representative image provided by Dr. Kara Duffy (unpublished, 2005).

3.3.3 Treatment Groups

Three treatment groups were used in the study: 24 μ L of acidic saline, 120 μ g insulin dissolved in 24 μ L, and a combination of 120 μ g insulin and 60 μ g PGZ dissolved in 24 μ L (PGZ+Insulin) (Renner et al., 2012).

The Saline treatment group was used as a control. PGZ+Insulin was administered because TZDs had been shown to upregulate insulin receptors (Searcy et al., 2012). Combining insulin with PGZ would reduce the likelihood that insulin levels act as a limiting factor to the effects of PGZ. Because the PGZ+Insulin treatment included insulin, an Insulin only treatment group was administered to determine if any changes in glucose metabolism and pathology were attributed to solely insulin or insulin sensitization by PGZ.

3.3.4 Study Phases

Forty-five mice were grouped into three cohorts of 15 mice based on age to control for degree of pathology. Three treatment groups (Saline, Insulin, and PGZ+Insulin) were used within each phase (n=5) (Figure 10). Phases varied both in treatment duration as well as time between treatment completion and sacrifice.

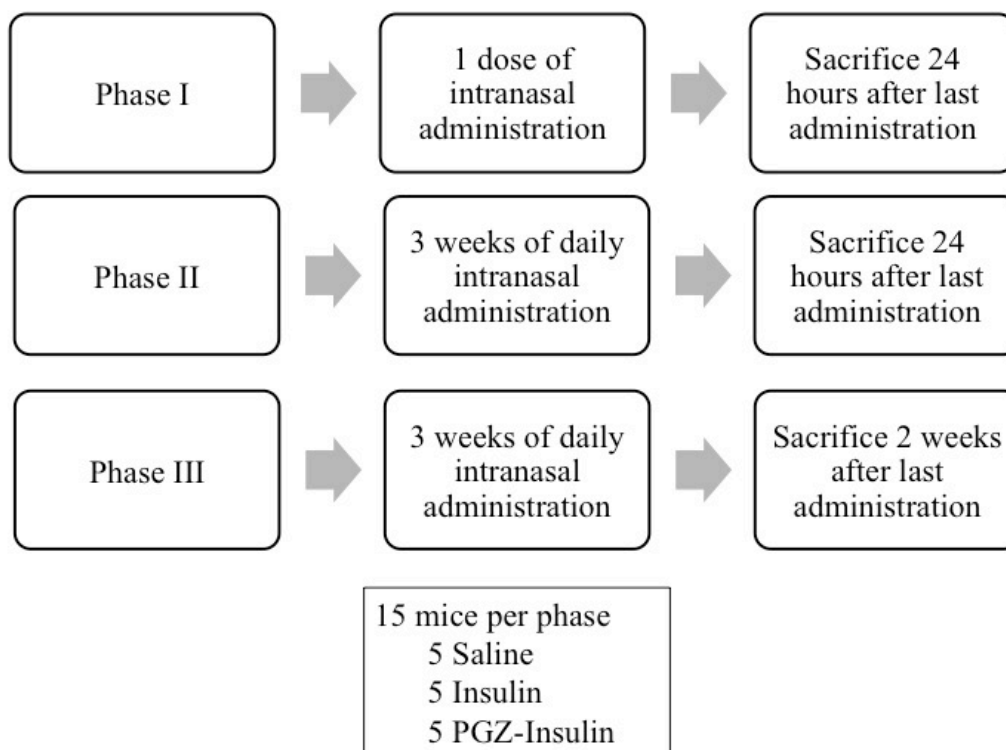


Figure 10. *Phases in Main Study.* A schematic of the phases used in this study. Created by I. Green.

The aim of Phase I was to validate that 3x-Tg-AD mice would be affected by the intranasal dosing method similarly to the non-transgenic mice in the Pilot Study. Mice were administered one intranasal treatment, and samples were collected 24 hours after administration.

The aim of Phase II was to observe the effects of a long-term intranasal treatment on AD pathology as well as brain glucose metabolism. Mice were administered intranasal treatment daily for three weeks, and samples were collected 24 hours after the last administration.

The aim of Phase III was to observe the lasting effects of long-term intranasal treatment on AD pathology and brain glucose metabolism. Mice were administered intranasal treatment daily for three weeks, and samples were collected two weeks after the last administration.

3.3.5 Immunohistochemistry Antibodies

In order to measure pathological hallmarks of AD, IHC tests were performed using antibodies specific to pathological targets, and then were visualized with light microscopy. A β plaque load can be measured through IHC, using the 6E10 antibody to quantify amyloid deposition (Gupta et al., 2014). AT-8 is a phosphorylation-specific tau antibody used in IHC to test for the presence of PHF-tau (Koga, Kojima, Kuwabara & Yoshiyama, 2014). As another hallmark of AD, microglial activation is often measured to quantify inflammation in the brain. This can be done through IHC tests using anti-Ionizing calcium-binding adaptor molecule 1 (Iba1) antibody, which measures activation of microglia (Koga et al., 2014; Gupta et al., 2014).

3.3.6 Fluxomics

Fluxomics analysis was used in the study to determine whether the rate of glucose metabolism was affected by the experimental treatments. Fluxomics is the study and quantitative measurement of the rate of metabolic reactions in cells, tissues, or organs during cell processes (Griffin, 2006). Fluxomics utilizes stable isotope labeling to measure the quantities of metabolites present at a specific moment during a metabolic process. In fluxomics, an organism can be labeled with a stable isotope such as ^{13}C (Niittylae, Chaudhuri, Sauer & Frommer, 2009). Then, gas

chromatography-mass spectrometry (GC-MS) can be used to analyze tissue to measure quantities of metabolites present during a metabolic process. A pattern-recognizing computer program identifies the metabolic phenotype of a genetic modification by separating the metabolic changes associated with the modification or cell process from the already existing metabolic variations of an organism, therefore providing information on the metabolic activity (Griffin, 2006).

Chapter 4: Methodology

4.1 Animal Care

All animal procedures were submitted to and approved by the IACUC in the spring of 2014, and mice were handled in accordance with the University of Maryland and Animal Care guidelines (Appendix B). Mice were acclimated to their surroundings and to the team members performing the procedure for several weeks prior to study execution. For more information about the living environment of the mice, see Appendix B.

4.2 Intranasal Administration

Treatments were administered intranasally by dripping treatment into each mouse's nostrils with a Hamilton syringe. Appendix C details the intranasal grip method used to immobilize the mice during administration. This method was an alternative to frequent anesthetization, reducing stress and unwanted side effects. Treatment drops were administered to alternating nostrils, allowing enough time for each nostril to clear before proceeding to the next (Renner et al., 2012). In order to administer PGZ intranasally, a diluted saline solution of PGZ was made manually by dissolving 60 μg , the optimal dose determined through the Pilot Study, into acidic saline. A detailed explanation of the intranasal administration method can be found in Appendix C.

4.3 Sample Collection

Stable isotope labeling was used to assess potential changes in glucose metabolism between treatment groups. Two hours before sacrificing, ^{13}C glucose tracer was injected intraperitoneally into mice. Injecting and sacrificing procedures were staggered to ensure that the tracer remained in each mouse for no more or less than two hours. ^{13}C glucose tracer was then detected via post-mortem fluxomics analysis of brain samples.

In accordance with an approved IACUC protocol, animals were humanely euthanized and tissue samples were collected for analysis. After decapitation, blood was collected and brains were removed within minutes of death (Spijker, 2011). Brains were then hemisected. The left hemisphere was frozen and stored at -80°C for future metabolic analysis. The right hemisphere was fixed in 10% formalin for 72 hours and then moved to fresh 1x phosphate buffered saline (PBS). Fixed tissue was paraffin embedded and sagittal sections were prepared (American Histolabs, Gaithersburg MD). Slides were later processed using immunostaining methods (Shankar et al., 2009).

4.4 Immunohistochemistry

6E10 ($\text{A}\beta$ deposition), Iba1 (microgliosis), and AT8 (PHF-tau) antibodies were used, and modified staining procedure was performed to identify immunoreactivity in the subiculum (Gupta et al., 2014; Koga et al., 2014). Regions of interest were delineated based on anatomical landmarks identified using a mouse

stereotaxic atlas (Paxinos, Watson, & Emson, 1980). Primary antibodies included a mouse 6E10 antibody (1:300, Covance Inc., Princeton NJ), rabbit Iba1 antibody (1:150, Wako Chemicals USA, Richmond VA), and human AT8 antibody (1:100, Thermo Fisher Scientific, Waltham, MA).

Slides were deparaffinized in xylene and hydrated in graded ethanol prior to antibody staining. Following permeabilization and blocking, tissue sections were incubated with primary antibodies and followed with appropriate biotinylated secondary antibodies (Vector Labs, Burlingame CA). Vectastain ABC kit (Vector Labs, Burlingame CA) was applied to slides and Vector DAB peroxidase substrate kit (Vector Labs, Burlingame CA) was utilized to view labeled protein in regions of interest. Additional IHC controls were included to exclude nonspecific staining due to interference from secondary mouse antibodies from analysis. Slides were then counterstained with hematoxylin to visualize nuclei. Slides were mounted using Vectamount permanent mounting medium (Vector Labs, Burlingame CA) and left overnight to dry before imaging.

4.5 Image Analysis

After IHC staining to identify proteins of interest, brain slices were examined and imaged using a Zeiss AxioObserver.Z1 (Zeiss, Germany) microscope (2.5x Objective, 0.07 aperture) to assess AD pathology. IHC endpoints were analyzed in the subiculum region of the hippocampus. Images were captured using ZEN 2012 software (Zeiss, Germany) using uniform hardware and software settings.

Trained observers identified positive staining for each antibody. 6E10 positive staining was counted for two micrographs from each animal. Counts were averaged to determine differences between groups for each study phase. Trained observers also examined slides and semi-quantified both AT8 and Iba1 staining using a Likert scale. A three-point Likert scale was developed to include rankings of “low”, “medium”, and “high” levels of staining corresponding to scores of 1, 2, and 3 respectively (Appendices E and F). This three-category quantification scheme was used because the nature of the Iba1 and AT8 staining was not conducive to counting discrete units, so a more general means of quantification was necessary. To combat the subjective nature of ranking with a Likert scale, images were ranked by 12 individuals and averages were taken.

4.6 Statistics

After the IHC results were quantified, a two-way statistical test was used to determine whether changes between treatment groups were statistically significant. The Kruskal-Wallis is a nonparametric test that analyzes the variance between three or more independently sampled groups and allows for different sample sizes (McKnight & Najab, 2010). Due to the nature of data scored with the Likert scale, nonparametric statistical tests were needed to analyze the AT8 and Iba1 assays. A normal distribution for 6E10 assay data could not be assumed, thus a nonparametric test was required for this data as well. If the differences were found to be significant, a Steel-Dwass test was then used to make pairwise comparisons between each of the three treatments (Neuhäuser & Bretz, 2001).

Due to small sample sizes, and in order to decrease probability of Type I error, statistical significance was established at the $\alpha=0.1$ level for all tests. Means and standard errors were calculated and graphed for each treatment group.

4.7 Luminescence Assay

Caspase 3/7 and Caspase 9 assays were performed to measure apoptosis. Frozen brains were thawed on ice in T-Per buffer (Thermo Scientific, Waltham MA) containing a protease inhibitor cocktail (Sigma-Aldrich, St. Louis MO) for tissue homogenization. Homogenates were analyzed for Caspase 3/7 and Caspase 9 activity according to the manufacturer's standard protocol (Promega, Madison, WI). Briefly, a 25 μ L sample was mixed gently for 30s with 25 μ L Caspase-Glo 3/7 reagent in white-walled 96-well plates and incubated for 2h at room temperature in the dark. Lysis buffer with the caspase reagent served as a blank. All samples were run in duplicate. Luminescence was measured using a FLUOstar Omega microplate reader (BMG Labtech, Cary NC) and values were expressed as relative intensity units (RIU) to compare between groups for each phase of study.

4.8 Fluxomics

¹³C glucose tracer was injected intraperitoneally in mice before sacrificing. This tracer was used to indicate the rate of glucose metabolism in the brain. Brain samples were homogenized, followed by the use of chloroform to remove lipids from the sample. Proteins were pelleted out and the aqueous supernatant was blown down

under nitrogen to isolate glucose. Following glucose extraction and separation, Di-O-isopropylidene Acetate (IPAc) derivatives of hexoses were acetylated, ensuring that the samples could be analyzed using GC-MS (Hachey, Parsons, McKay & Haymond, 1999). For a complete version of the used protocol, see Appendix F.

Chapter 5: Results

Results were obtained from three post-mortem IHC tests, luminescence assays, and fluxomics analysis.

5.1 Immunohistochemistry

5.1.1 6E10 (A β plaque)

3x-Tg-AD mice were divided by intranasal treatment with groups of Saline, Insulin, or PGZ+Insulin. 6E10 immunoreactivity was counted in the subiculum to assess amyloid deposition in each phase of study. In Phase I (Figure 11), samples were collected 24 hours after a single treatment. Mean amyloid deposition count for Saline was 0.50 ± 0.079 , mean count for Insulin was 3.0 ± 1.2 , and mean count for PGZ+Insulin was 1.5 ± 0.84 . Observed 6E10 immunoreactivity was similar across groups and statistical analysis was not significant, ($p=0.222$, $\chi^2(2)=3.01$)

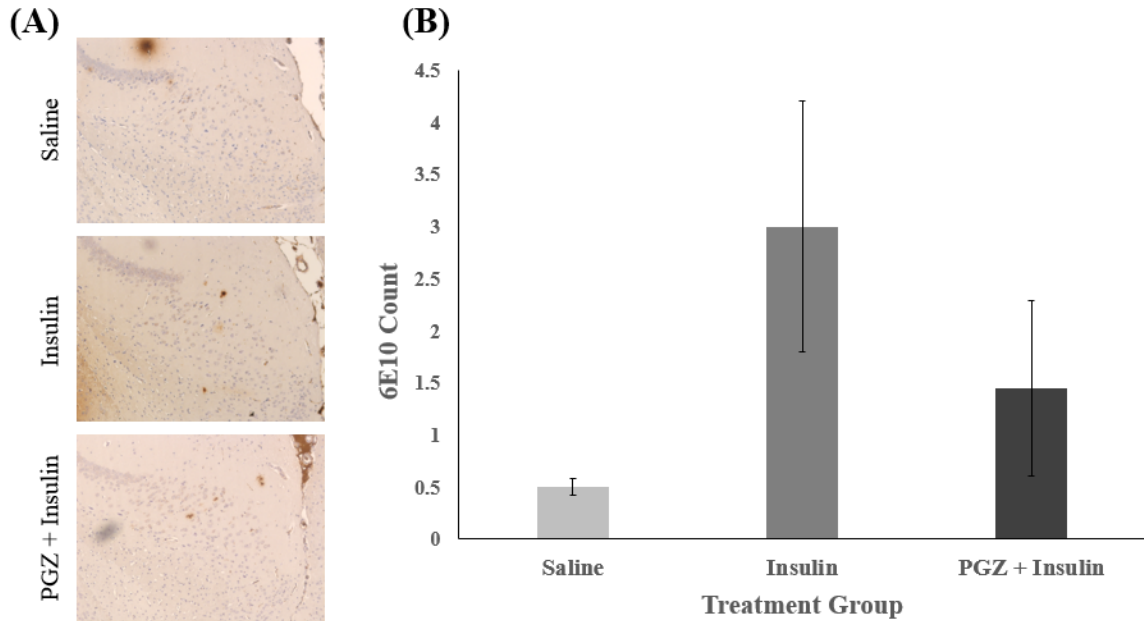


Figure 11. Amyloid Deposition Phase I. (A) Representative images of 6E10 immunostaining in the subiculum of 3x-Tg-AD mice from each treatment group. (B) Pathology was quantified and histogram depicts mean \pm standard error of the mean (SEM) amyloid deposition. Statistical analysis revealed no significant differences ($p=0.222$, $\chi^2(2)=3.01$).

In Phase II (Figure 12), samples were collected 24 hours after three weeks of daily treatment. Mean count for Saline was 21.2 ± 7.2 , mean count for Insulin was 14.3 ± 4.9 , and mean count for PGZ+Insulin was 3.6 ± 1.4 . A Kruskal-Wallis test was significant ($p=0.038$, $\chi^2(2)=6.52$) and a post hoc test using pairwise comparisons yielded significance for Saline vs. PGZ+Insulin ($p=0.056$), but not for Saline vs. Insulin ($p=0.806$) or PGZ+Insulin vs. Insulin ($p=0.212$).

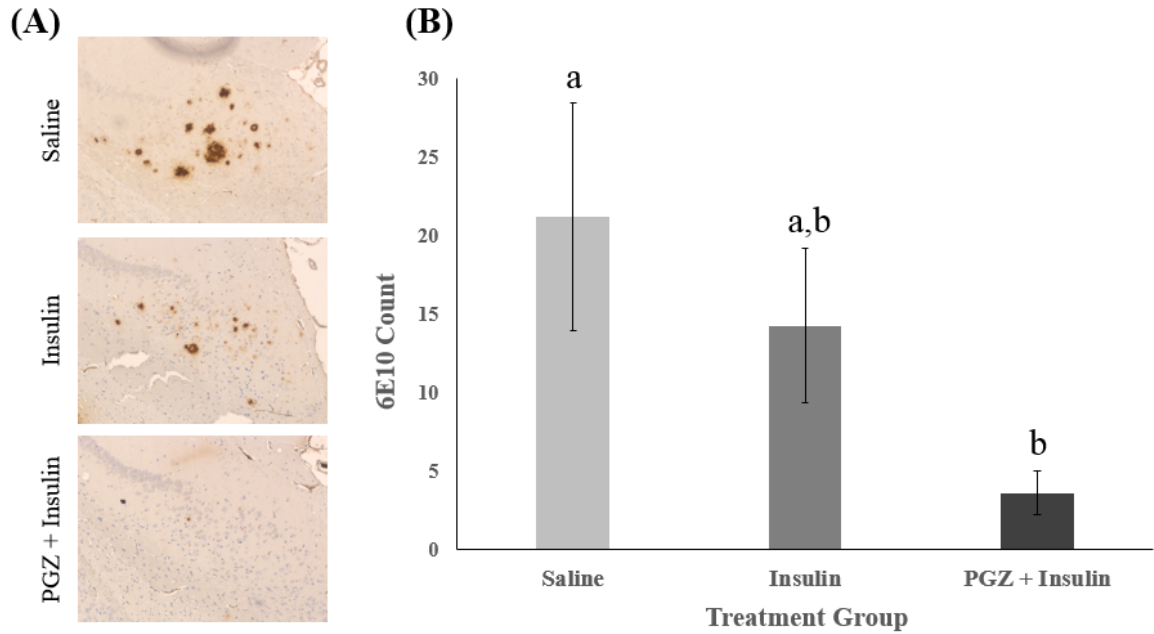


Figure 12. Amyloid Deposition Phase II. (A) Representative images of 6E10 immunostaining in the subiculum of 3x-Tg-AD mice from each treatment group. (B) Pathology was quantified and histogram depicts mean \pm SEM amyloid deposition. Statistical analysis revealed significant group differences ($p=0.038$, $\chi^2(2)=6.52$). Post hoc tests revealed significant difference between Saline (a) and PGZ+Insulin (b) treatment groups ($p=0.056$).

In Phase III (Figure 13), samples were collected two weeks after three weeks of daily treatment. Mean count for Saline was 19.6 ± 4.5 , mean count for Insulin was 4.8 ± 3.2 , and mean count for PGZ+Insulin was 5.1 ± 2.2 . A Kruskal-Wallis test was significant ($p=0.035$, $\chi^2(2)=6.71$) and a post hoc test using pairwise comparisons yielded significance for Saline vs. PGZ+Insulin ($p=0.056$) but not for Saline vs. Insulin ($p=0.145$) or PGZ+Insulin vs. Insulin ($p=0.860$).

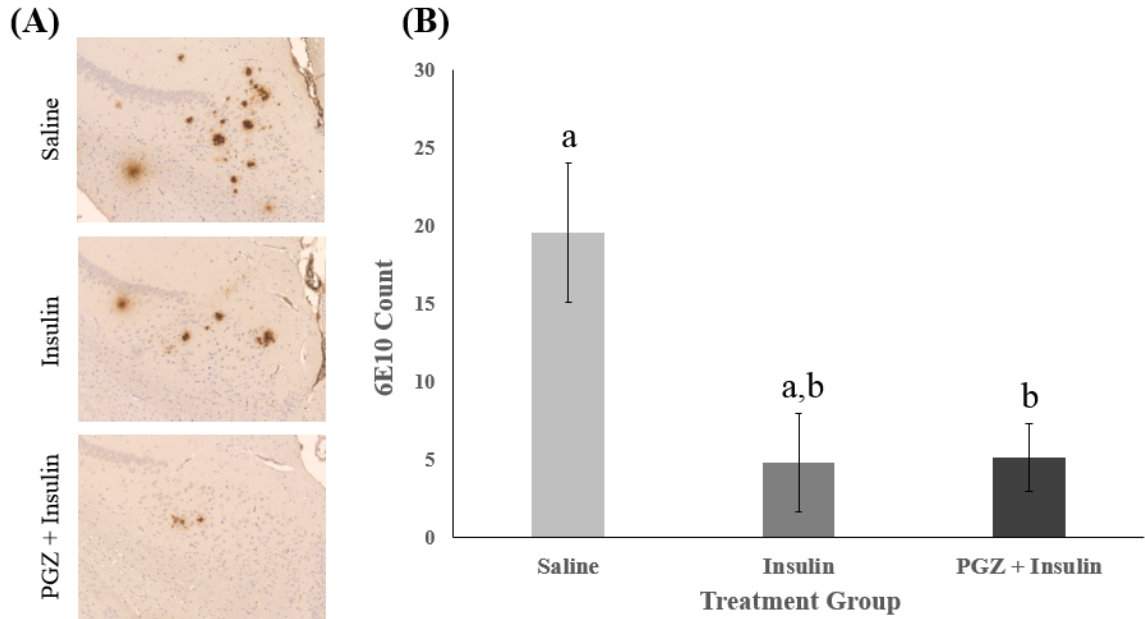


Figure 13. Amyloid Deposition Phase III. (A) Representative images of 6E10 immunostaining in the subiculum of 3x-Tg-AD mice from each treatment group. (B) Pathology was quantified and histogram depicts mean \pm SEM amyloid deposition. Statistical analysis revealed significant group differences ($p=0.035$, $\chi^2(2)=6.71$). Post hoc tests revealed significant difference between Saline (a) and PGZ+Insulin (b) treatment groups ($p=0.056$).

5.1.2 Iba1 (Inflammation)

Another IHC test performed was Iba1 for activated microglia. Iba1 levels were quantified using a Likert scale in the subiculum to assess inflammation in each phase of the study. In Phase I (Figure 14), samples were collected 24 hours after a single treatment. Mean rating for Saline was 1.1 ± 0.078 , mean rating for Insulin was 1.2 ± 0.20 , and mean rating for PGZ+Insulin was 1.3 ± 0.14 . Observed Iba1

immunoreactivity was similar across groups and statistical analysis was not significant ($p=0.361$, $\chi^2(2)=2.04$).

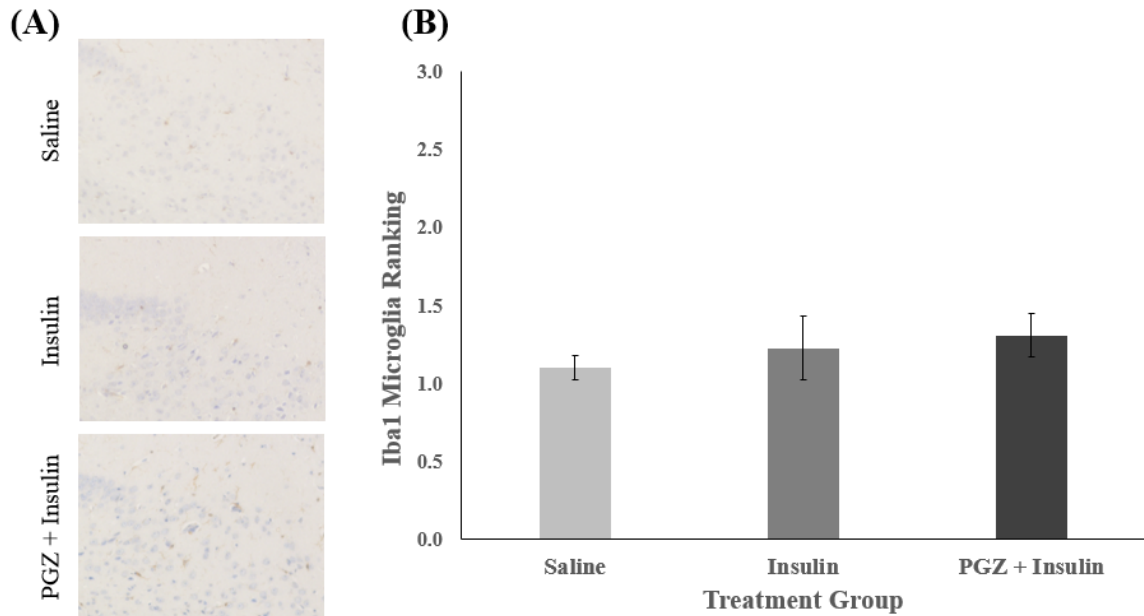


Figure 14. *Iba1* Activated Microglia Ranking Phase I. (A) Representative images of *Iba1* immunostaining in the subiculum of 3x-Tg-AD mice from each treatment group. (B) Pathology was quantified and histogram depicts mean \pm SEM inflammation rating. Statistical analysis revealed no significant differences ($p=0.361$, $\chi^2(2)=2.04$).

In Phase II (Figure 15), samples were collected 24 hours after three weeks of daily treatment. Mean rating for Saline was 2.5 ± 0.21 , mean rating for Insulin was 1.4 ± 0.14 , and mean rating for PGZ+Insulin was 1.1 ± 0.14 . A Kruskal-Wallis test was significant ($p=0.0054$, $\chi^2(2)=10.45$) and a post hoc test using pairwise comparisons

yielded significance for Saline vs. Insulin ($p=0.056$) and Saline vs. PGZ+Insulin ($p=0.026$) but not for PGZ+Insulin vs. Insulin ($p=0.196$).

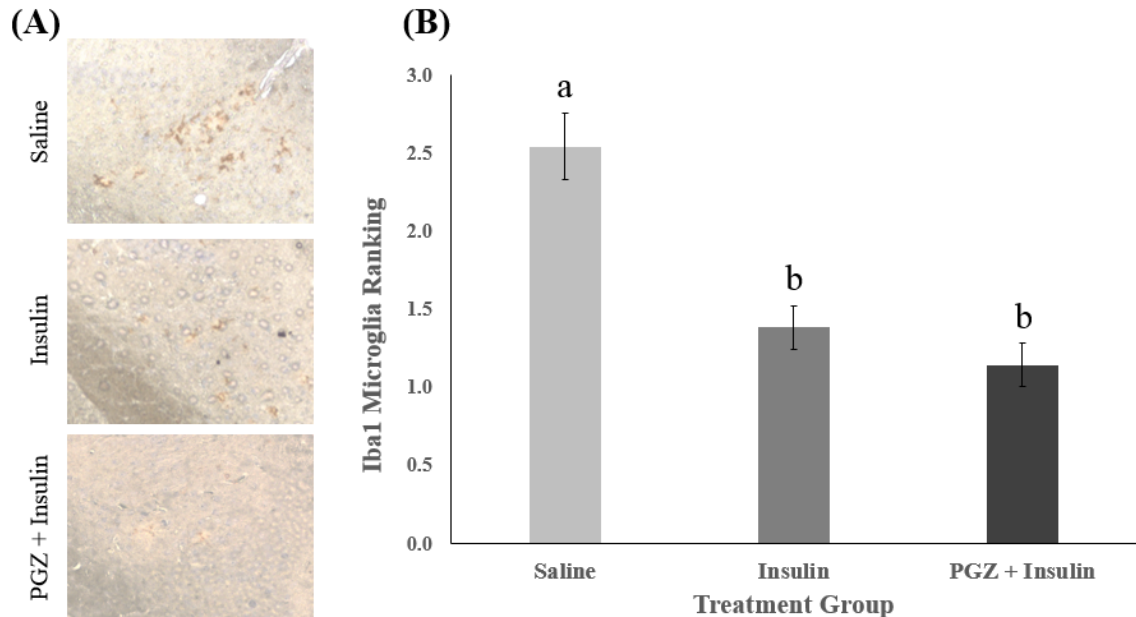


Figure 15. *Iba1* Activated Microglia Ranking Phase II. (A) Representative images of *Iba1* immunostaining in the subiculum of 3x-Tg-AD mice from each treatment group. (B) Pathology was quantified and histogram depicts mean \pm SEM inflammation rating. Statistical analysis revealed significant group differences ($p=0.0054$, $\chi^2(2)=10.45$). Post hoc tests revealed significant difference between Saline (a) and Insulin (b) treatment groups ($p=0.056$) and Saline (a) and PGZ+Insulin (b) treatment groups ($p=0.026$).

In Phase III (Figure 16), samples were collected two weeks after three weeks of daily treatment. Mean rating for Saline was 2.8 ± 0.071 , mean rating for Insulin was 1.4 ± 0.25 , and mean rating for PGZ+Insulin was 1.8 ± 0.35 . A Kruskal-Wallis test was

significant ($p=0.027$, $\chi^2(2)=7.23$) and a post hoc test using pairwise comparisons yielded significance for Saline vs. Insulin ($p=0.030$) but not for Saline vs. PGZ+Insulin ($p=0.258$) or PGZ+Insulin vs. Insulin ($p=0.731$).

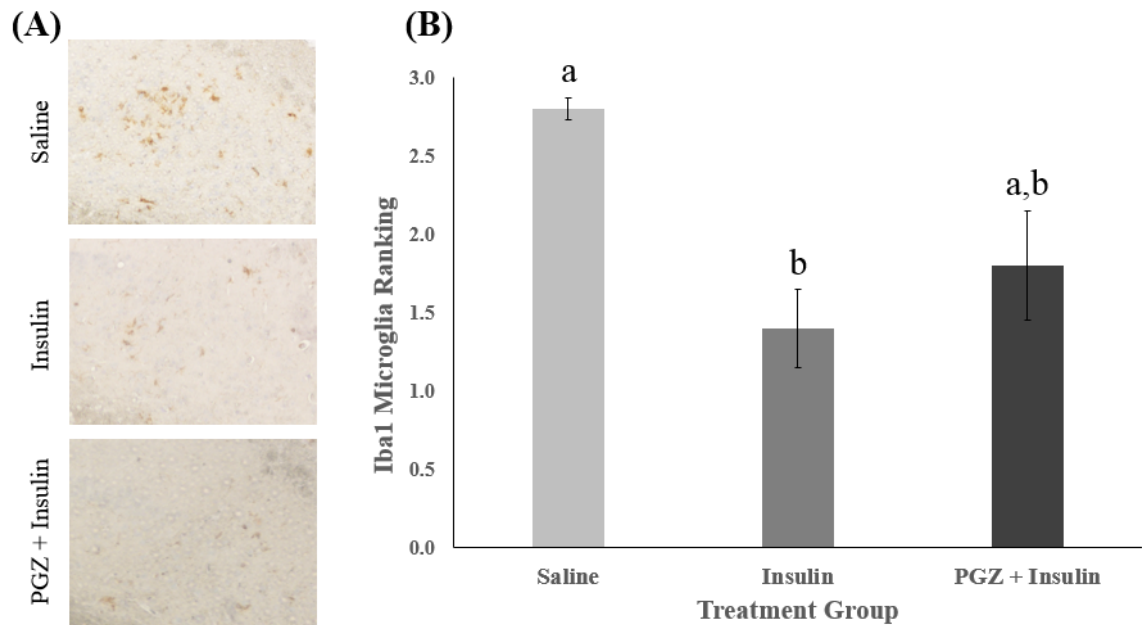


Figure 16. *Iba1* Activated Microglia Ranking Phase III. (A) Representative images of *Iba1* immunostaining in the subiculum of 3x-Tg-AD mice from each treatment group. (B) Pathology was quantified and histogram depicts mean \pm SEM inflammation rating. Statistical analysis revealed significant group differences ($p=0.027$, $\chi^2(2)=7.23$). Post hoc tests revealed significant difference between Saline (a) and Insulin (b) treatment groups ($p=0.030$).

5.1.3 AT8 (PHF-tau)

Another IHC test performed was AT8 immunostaining. AT8 levels were quantified using a Likert scale in the subiculum to assess PHF-tau prevalence in each phase of the study. In Phase I (Figure 17), samples were collected 24 hours after a single treatment. Mean rating for Saline was 1.4 ± 0.065 , mean rating for Insulin was 1.8 ± 0.36 , and mean rating for PGZ+Insulin was 1.3 ± 0.12 . Observed PHF-tau immunoreactivity was similar across groups and statistical analysis was not significant ($p=0.435$, $\chi^2(2)=1.67$).

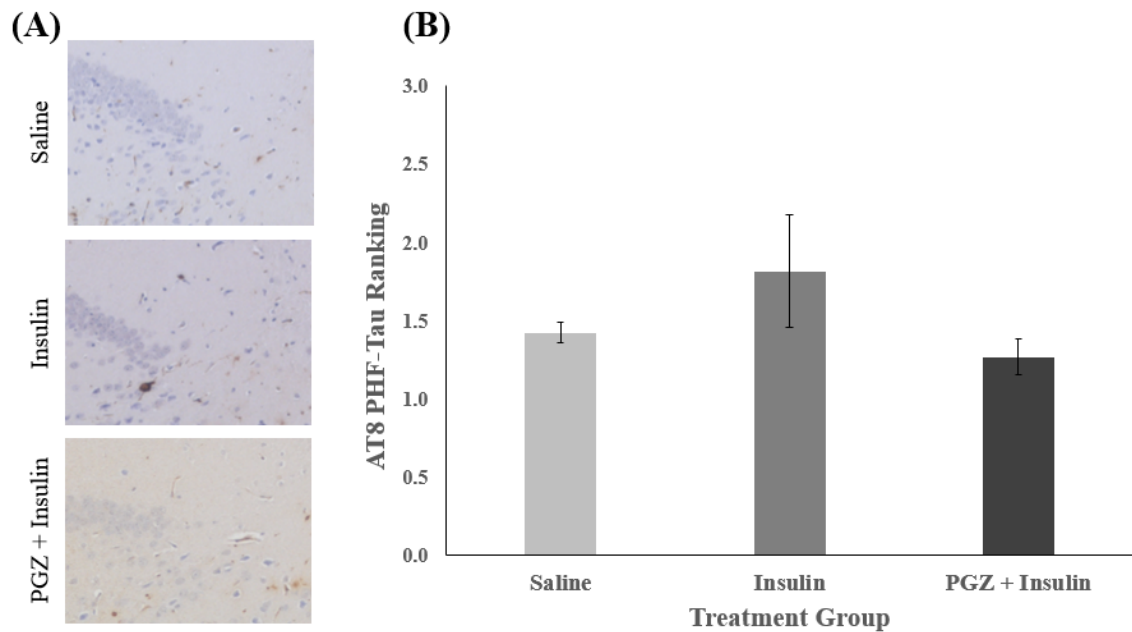


Figure 17. AT8 PHF-Tau Phase I. (A) Representative images of AT8 immunostaining in the subiculum of 3x-Tg-AD mice from each treatment group. (B) Pathology was quantified and histogram depicts mean \pm SEM PHF-Tau rating. Statistical analysis revealed no significant differences ($p=0.435$, $\chi^2(2)=1.67$).

In Phase II (Figure 18), samples were collected 24 hours after three weeks of daily treatment. Mean rating for Saline was 2.3 ± 0.11 , mean rating for Insulin was 2.4 ± 0.16 , and mean rating for PGZ+Insulin was 2.3 ± 0.11 . Observed PHF-tau immunoreactivity was similar across groups and statistical analysis was not significant ($p=0.810$, $\chi^2(2)=0.422$).

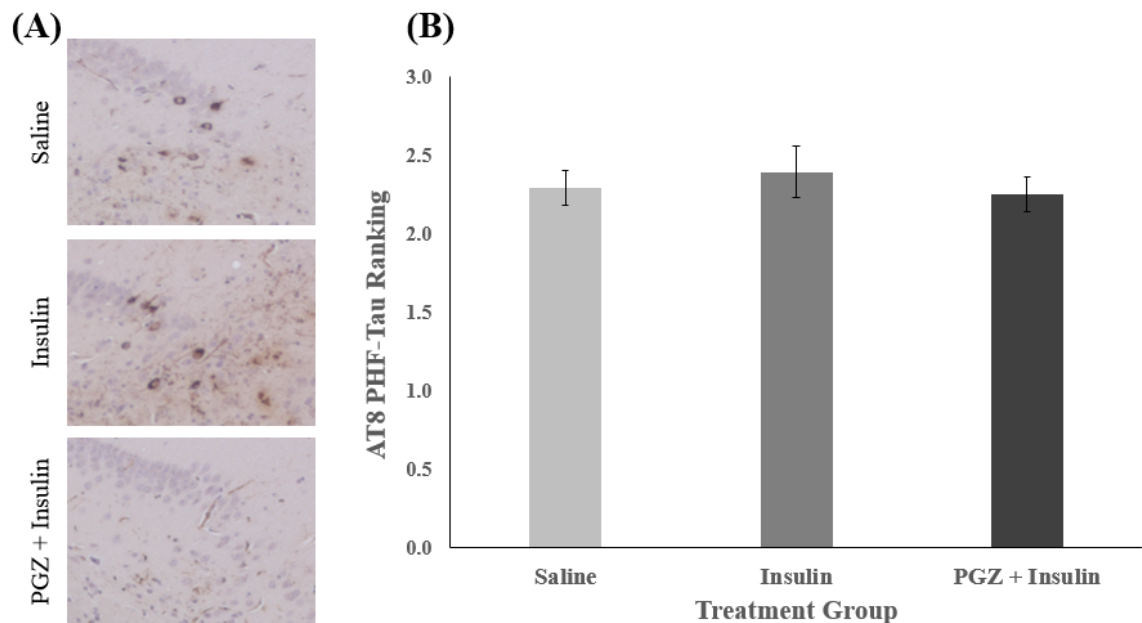


Figure 18. AT8 PHF-Tau Phase II. (A) Representative images of AT8 immunostaining in the subiculum of 3x-Tg-AD mice from each treatment group. (B) Pathology was quantified and histogram depicts mean \pm SEM PHF-Tau rating. Statistical analysis revealed no significant differences ($p=0.810$, $\chi^2(2)=0.422$).

In Phase III (Figure 19), samples were collected two weeks after three weeks of daily treatment. Mean rating for Saline was 2.0 ± 0.11 , mean rating for Insulin was

1.8±0.064, and mean rating for PGZ+Insulin was 2.1±0.093. Observed PHF-tau immunoreactivity was similar across groups and statistical analysis was not significant ($p=0.110$, $\chi^2(2)=4.41$).

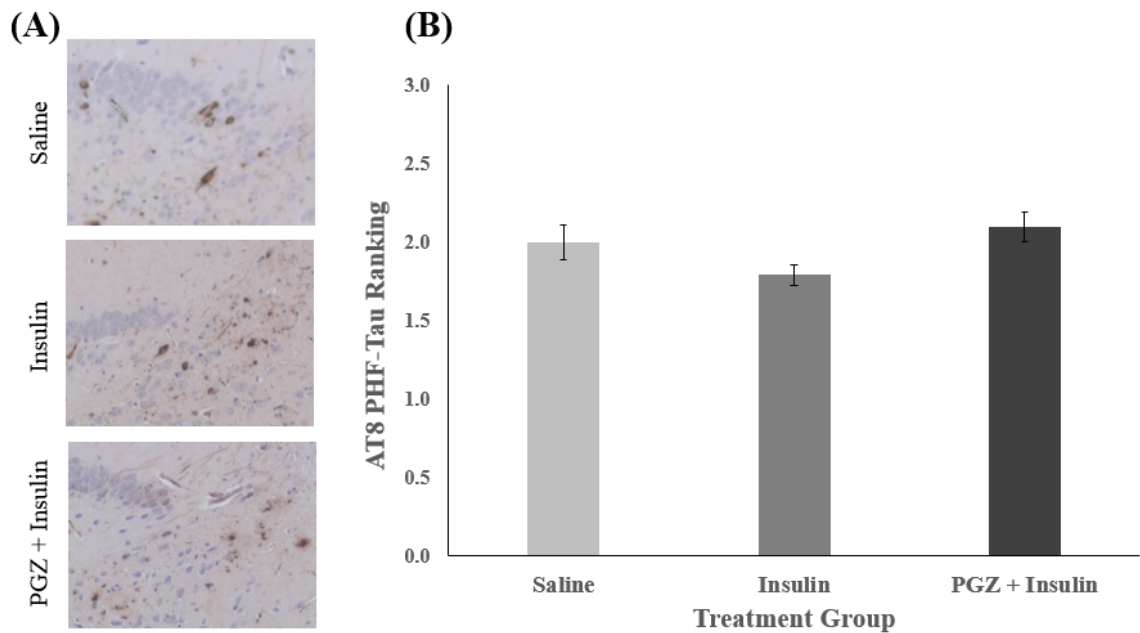


Figure 19. AT8 PHF-Tau Phase III. (A) Representative images of AT8 immunostaining in the subiculum of 3x-Tg-AD mice from each treatment group. (B) Pathology was quantified and histogram depicts mean \pm SEM PHF-Tau rating. Statistical analysis revealed no significant differences ($p=0.110$, $\chi^2(2)=4.41$).

5.2 Luminescence Assays

In carrying out the luminescence assays, the majority of samples in each phase were below the detection limit of Caspase 3/7 and Caspase 9. Thus, resulting data was not interpretable, and further analysis was not performed.

5.3 Fluxomics

Phase II and Phase III fluxomics data was processed, however, it was lost due to GC-MS computer failure before it was able to be analyzed. A different GC-MS machine was used to process the Phase I samples, and fluxomics data was obtained. As of publication time, the process of identifying the glucose in the fluxomics data has not yet been completed. A standard is necessary to determine the expected fluxomics response of the labeled glucose, which will enable the location of potential glucose peaks in the fluxomics data for Phase I to be identified. Once this is completed, the fluxomics data will be able to be analyzed to determine the effect of the intranasal treatments on glucose uptake. Therefore, further statistical analysis has not yet been performed for Phase I fluxomics data.

Chapter 6: Discussion

The goal of this study was to investigate the effects of intranasal administration of PGZ+Insulin on a 3x-Tg-AD mouse model. Three phases were conducted to test various lengths of treatment, as well as short and long-term waiting periods between treatment and sacrifice. Fluxomics analysis of Phase I was expected to show elevated glucose uptake in the PGZ+Insulin treatment, followed by a slight increase in glucose uptake in the Insulin only group. In the long-term treatment phases of the study, Phases II and III, the PGZ+Insulin treatment was expected to decrease AD pathology more than an Insulin treatment alone, and both of these treatment groups were expected to exhibit less pathology than the Saline treatment. AD pathology was measured using IHC targeting A β deposits, PHF-tau, and activated microglia. Glucose metabolism was measured using fluxomics analysis and caspase activity was measured using luminescence assays.

In Phase I, a single dose of each treatment (Saline, Insulin, and PGZ+Insulin) was administered to mice that were then sacrificed 24 hours post-treatment. This phase was designed to investigate the effects of intranasal administration of treatments on brain glucose metabolism in 3x-Tg-AD mice.

As no detectable ^{13}C sample was found through Phase I fluxomics results, it is hypothesized that the increased glucose observed in the Pilot Study after immediate sacrifice of one intranasal PGZ+Insulin administration also took place in the 3x-Tg-AD mice in Phases I, II, and III.

Analysis of pathological endpoints showed low levels of AD pathology (amyloid depositions, PHF-tau, and activated microglia) in each treatment group, with high variance among groups and no significant differences across treatment groups. Observations of mean counts suggest that fewer A β plaques were observed in Phase I treatment groups compared to treatment groups in Phases II and III. Age could be responsible for this difference since the Phase I mice were 9-11 months of age, and consistent levels of A β were expected at 12 months of age for this colony of mice (personal communication, K. Duffy). Additionally, since mice received a single dose prior to sacrifice, a 24-hour window was likely not long enough to allow for changes in protein levels resulting from insulin signaling alterations. PGZ achieves steady-state serum concentrations within seven days, so the amount of PGZ after 24 hours was likely not enough to significantly affect AD pathology in the model (National Institutes of Health, 2009).

In addition, as the luminescence assays provided no observable sample, no further analysis was performed. Therefore, no conclusions or observations about apoptosis could be made for any phase in this study.

In Phase II, mice aged 15-17 months old were administered treatment daily for a period of three weeks, and were sacrificed 24 hours after the last administration. In Phase III, mice aged at 14 months were also dosed daily for three weeks, but pathology was assessed two weeks after the last administration of treatment. These phases were designed to investigate the immediate and persistent effects of a longer-term regimen of intranasal treatments on brain glucose metabolism and AD pathology in 3x-Tg-AD mice.

Results of IHC did not show significant differences between Insulin and PGZ+Insulin treatment groups across Phase II and Phase III as hypothesized. However, there may be factors associated with experimental design and methodology that could have attributed to the lack of significant difference. One main factor was small sample size, as having 5 mice per treatment group decreased likelihood of significant results. Additionally, previous literature indicated that there should have been a significant difference in AD pathology when administering intranasal insulin (Liu et. al., 2013). However, this was not seen in many of the results, suggesting that higher concentrations of insulin and PGZ may have been needed in order to see more significant effects. Considering such limiting factors, further discussion points and proposed pathways were based on preliminary observations and trends seen in data in addition to any significant differences found in results.

Due to loss of fluxomics data for Phases II and III, conclusions could not be drawn from Main Study samples. Conclusions about glucose metabolism were drawn from Pilot Study data instead. Increased glucose uptake from a PGZ+Insulin treatment was observed in non-transgenic mice in the Pilot Study; it was therefore expected that similar effects would be seen in 3x-Tg-AD mice in the Main Study. This increase in glucose uptake would address the theory of AD as “Type III Diabetes.” Insulin signaling is impaired in AD because of interference from A β oligomers and TNF α (Xie et al., 2002). Insulin triggers signaling molecules in the ISP, especially IRS1. With increased levels of IRS1, some downstream signaling is able to continue despite inference from TNF α , and more insulin is present to compete with A β as a signaling molecule (De Felice, Lourenco & Ferreira, 2014). As it is

hypothesized that AD neurons are insulin resistant, the increase in glucose metabolism by PGZ+Insulin and sensitization of insulin signaling through activation of PPAR γ would compensate for this decrease in glucose uptake. PGZ stimulates both PPAR γ and Akt to upregulate the translocation and transcription of GLUT4 (Leonardini et al., 2009). PPAR γ also stimulates the Cbl/CAP complex to further increase the amount of GLUT4 (Monsalve et al., 2013). Therefore, the otherwise declined rate of glucose uptake could be raised by PGZ+Insulin treatment sensitizing the ISP to insulin.

The loss of glucose uptake in the AD brain could be more focused on insulin-independent mechanisms like GLUT1 and GLUT3. In this case, the treatment of PGZ+Insulin to GLUT4 would be compensating for the loss of glucose transport in other GLUTs, meaning that the treatment does not directly address the downregulation of GLUT1 and GLUT3 but still alleviates its effects through enhancing the contributory mechanism of GLUT4. This suggests that if AD is in part caused by a decrease in glucose uptake, treatment with an insulin sensitizer can help alleviate its effects.

In contrast, a different explanation of the increase in glucose uptake through PGZ+Insulin treatment could be that GLUT4 is a direct contributor to AD. This would suggest that the ISP and GLUT4 could be a faulty pathway. These proposed mechanisms could suggest that GLUT4 may play a more important role in AD pathology than previously understood. This would also be supported by the discoveries of abundant GLUT4 mRNA in the subiculum and hippocampus, which are directly related to AD symptoms and pathology (El Messari et al., 2002).

Significant difference was found between Saline and PGZ+Insulin treatments groups in 6E10 data for Phase II. Additionally, general trends in mean counts show lower amyloid deposition counts in the PGZ+Insulin group than in the Insulin group for Phase II, indicating that the addition of PGZ lowered pathology more than just Insulin when observed immediately after treatment. This trend may be due to the effects of insulin and PGZ on IDE and ApoE. The presence of insulin triggers IDE, which degrades A β plaques (Farris et al., 2003). PGZ increases insulin's effects by sensitizing the cell, and it increases ApoE proteins that degrade A β plaques. The increased effect of PGZ on plaque amelioration may also be due to the drug's downregulation of the BACE1 enzyme that improperly cleaves APP and creates A β oligomers (Liu et al., 2013).

For Phase III 6E10 data, significant difference was found between Saline and PGZ+Insulin, similar to Phase II. However, in contrast to Phase II, data trends showed very little difference in mean counts between PGZ+Insulin and Insulin. This may suggest that the full effects of only insulin on A β plaques take longer to manifest, as Phase II saw a trend of decreased pathology in PGZ+Insulin compared to Insulin that was not observed in Phase III. However, because mean counts between PGZ+Insulin and Insulin seemed to become level in Phase III, it would suggest that the additive effects of PGZ are useful for a more immediate decrease in plaque formation but not for consistently decreased pathology compared to only insulin in the long term.

AT8 immunostaining for PHF-tau in both Phases II and III resulted in statistically insignificant differences between treatment groups. Both treatment

groups were expected to show a decline in pathology compared to the control. Insulin dysfunction results in increased phosphorylation of tau by inhibiting phosphatase activity (Planel et al., 2007). By restoring insulin signaling function, these effects were expected to subside. Insulin was also predicted to decrease the amount of hyperphosphorylation by inhibiting GSK-3, a kinase that hyperphosphorylates tau (Blazquez, Velazquez, Hurtado-Carneiro & Ruiz-Albusac, 2014). PGZ was predicted to cause an even greater reduction in pathology because of PPAR γ 's additional inhibitory effects on Cdk5 and JNK signaling.

Results from Iba1 immunostaining showed statistically significant differences between Insulin and Saline, as well as between PGZ+Insulin and Saline, in Phase II. In Phase III, significant difference was found only between Saline and Insulin treatment groups. The Insulin group was expected to show decreased inflammation because insulin modulates the PI₃K pathway responsible for inflammation and apoptosis in AD (Blazquez, Velazquez, Hurtado-Carneiro & Ruiz-Albusac, 2014). Insulin also inhibits GSK-3 activity, which stimulates the production of anti-inflammatory cytokines and decreases the amount of inflammatory cytokines (Blazquez, Velazquez, Hurtado-Carneiro & Ruiz-Albusac, 2014). PGZ was expected to have an effect on inflammation because the literature has shown that TZDs stop the transcription of AP-1 nuclear factor, thereby preventing microglial activation by A β plaques.

While a luminescence assay was performed to measure caspases 3,7 and 9 activity in Phase II and III, results were not interpretable due to samples in each phase being below detection level of caspase activity. This may have been due to a low

concentration of sample used in each well or a contaminated control well. Further testing needs to be completed to investigate the effect of PGZ+Insulin on apoptosis.

Chapter 7: Conclusion

AD has long been associated with complications in glucose metabolism. This study attempted to use PGZ in conjunction with insulin in order to activate PPAR γ and upregulate insulin receptors in order to increase glucose metabolism and decrease AD pathology (Figures 20 and 21). Insulin and PGZ+Insulin treatments were administered intranasally to 3x-Tg-AD mice in order to bypass the BBB and directly target treatment to the brain. Post-mortem analysis was performed in order to measure effects of treatment on brain glucose metabolism, A β plaques, NFTs, inflammation, and apoptosis. Pilot Study results indicated increase in glucose metabolism according to increasing doses of PGZ+Insulin, suggesting that the treatment would increase brain glucose metabolism in a 3x-Tg-AD mouse. While results were generally insignificant across post-mortem tests between PGZ+Insulin and Insulin treatments in the Main Study, general trends from A β deposition immunostaining may suggest that the addition of PGZ to insulin treatments would increase immediate effects on AD pathology, but would not enhance the effects of insulin treatments on AD pathology in the longer term. Thus, trends from the study and proposed biochemical pathways suggest that an intranasal PGZ+Insulin treatment could increase glucose metabolism and decrease pathology in an AD affected brain. Therefore, future research should continue to investigate the roles of TZDs and the ISP, especially through the use of intranasal administration of TZDs, in order to establish the pathways and causes involved in AD.

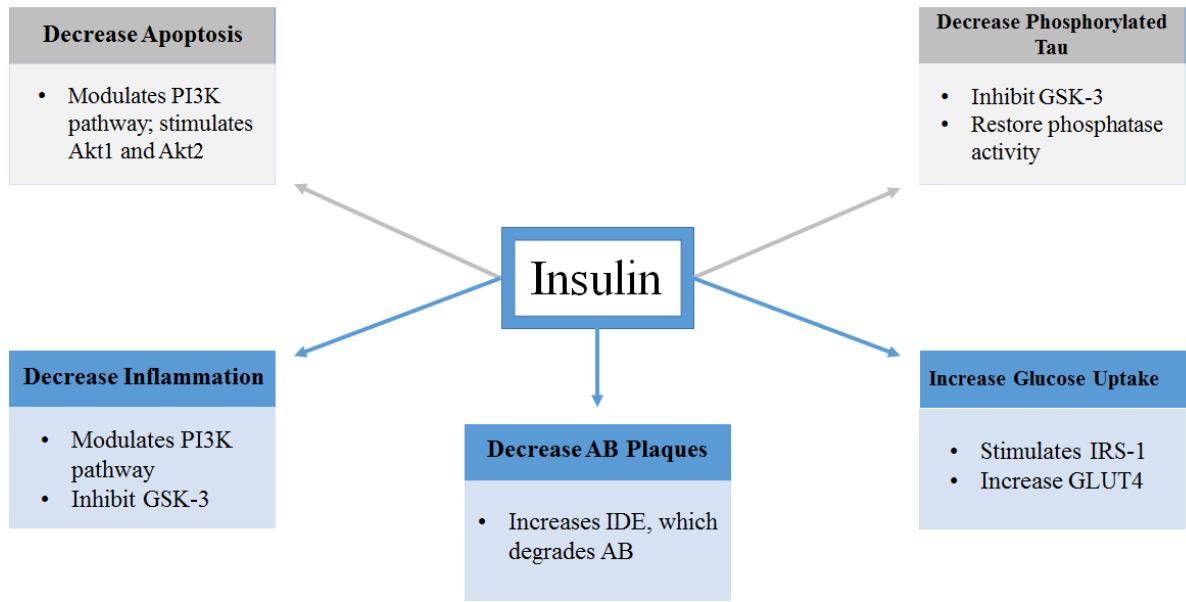


Figure 20. The Proposed Mechanisms by which the Insulin Treatment Ameliorates AD Pathology. *Decreased apoptosis and hyperphosphorylated tau was not observed in this study (grey). Insulin was shown to have an effect on inflammation, A β plaques, and glucose uptake (blue).* Figure modified from Perez & Quintanilla, 2015; De Felice, Lourenco, & Ferreira, 2014; Blazquez, Velazquez, Hurtado-Carneiro & Ruiz-Albusac, 2014; Farris et al., 2003; Leibiger, Leibiger & Berrgren, 2008. Created by A. Zachery.

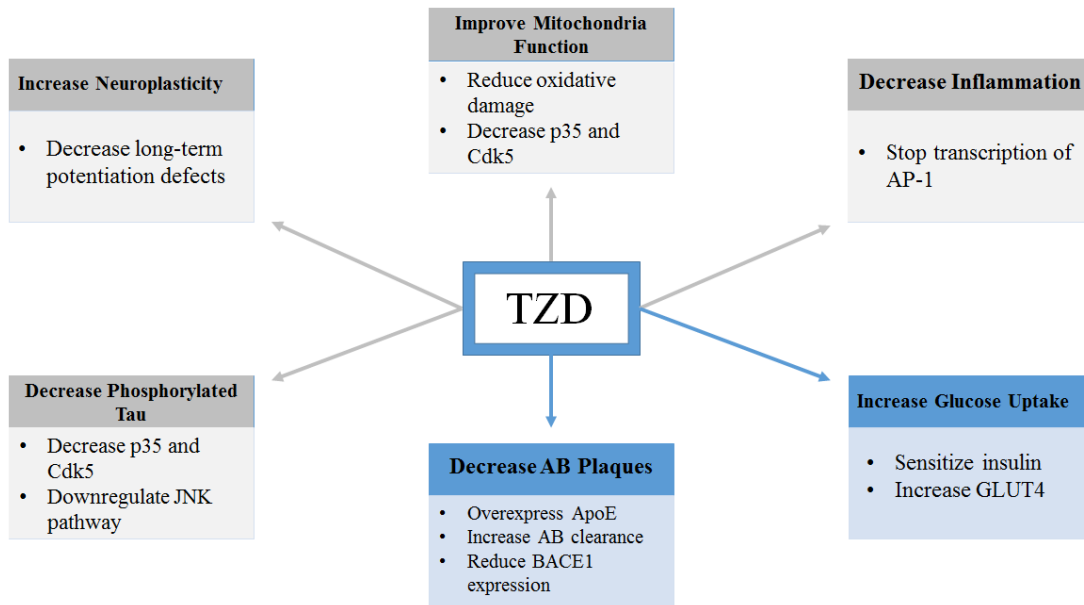


Figure 21. The Proposed Mechanisms by which the TZD Treatment Ameliorates AD Pathology. *Decreased apoptosis and hyperphosphorylated tau were not observed in this study, and mitochondria function and neuroplasticity was not investigated (grey). PGZ+Insulin was shown to have an additive effect over insulin treatment to reduce A β plaques and increase glucose uptake (blue).* Information from: Perez & Quintanilla, 2015 and Blazquez, Velazquez, Hurtado-Carneiro & Ruiz-Albusac, 2014. Created by A. Zachery.

7.1 Future Directions

The present study aimed to utilize the intranasal administration of PGZ in order to investigate the ISP in AD. Many of the results from the study were inconclusive or influenced by limiting factors and confounding variables. Further studies should be conducted that continue to focus on TZDs and AD in order to gain

more replicable data, robust results, and clearer insights into the role of the ISP and AD pathology.

As some of the techniques used were novel, future studies can aim to refine the methods used in this study. The largest obstacle of the present study was using the intranasal technique to administer PGZ, as there was no precedent in previous literature on standard dosing concentrations or solution preparation. Thus, it was challenging to discern if the results were caused by the effects of PGZ, or if the dose of PGZ was not high enough to see change. Future studies should aim to establish a standard protocol of the intranasal administration of PGZ in order to evaluate its effects on AD more vigorously.

Another obstacle faced in the present study was confounding variables across phases, which future studies should aim to reduce or eliminate. One of these confounding variables was the difference in mouse ages across study cohorts. For this study, it was not possible to compare results across phases, as each age group showed different levels of onset of AD pathology at the time of the treatment regimen. Future studies should isolate one age group across the entire study, or study the effects of an insulin and PGZ regimen across different age groups in order to evaluate the role of onset and level of pathology on the treatment. Another confounding variable was that during the dosing period, multiple researchers handled mice. This exposed the mice to varied durations of dosing and varied physical handling, which could have caused behavioral effects as well as effects on pathology. Finally, different GC-MS machines were used during fluxomics analysis across phases, resulting in calibrations differences of the machine, which could have

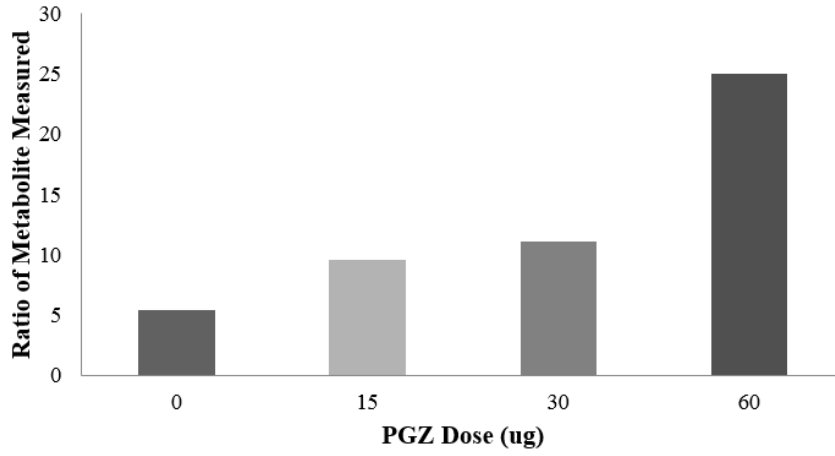
affected the resulting fluxomics data. Future experimental designs should aim to reduce such confounding variables.

In addition to changes in methodology, future studies could explore further theoretical designs of the present study to gain more information on the role of TZDs and the ISP on AD. For example, there are differences between the TZDs, PGZ and RGZ, and future studies could investigate the varying effects on AD pathology. Studies in the future could also conduct behavioral tests on animal models receiving a TZD and insulin regimen in order to investigate how changes in pathology translate into changes in observable behavior and memory. Additionally, it could be investigated whether the administration of a TZD alone, without combination with insulin, would affect AD pathology. This could indicate whether administration of TZDs coupled with insulin does in fact have an additive effect in comparison to administration of insulin or TZDs alone. Finally, studies could implement different time points than the present study to evaluate even longer term effects of a TZD and insulin regimen than the three weeks used in the current study. Performing future studies that address these different aspects can help further investigate the role of TZDs and the ISP on AD pathology in efforts to continue searching for the cause of and cure for AD.

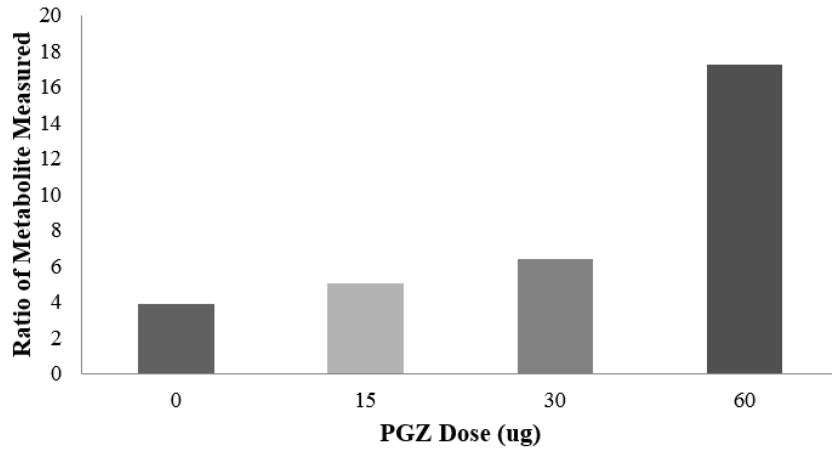
Appendices

Appendix A: Pilot Results

Pilot: Alanine



Pilot: Aspartate



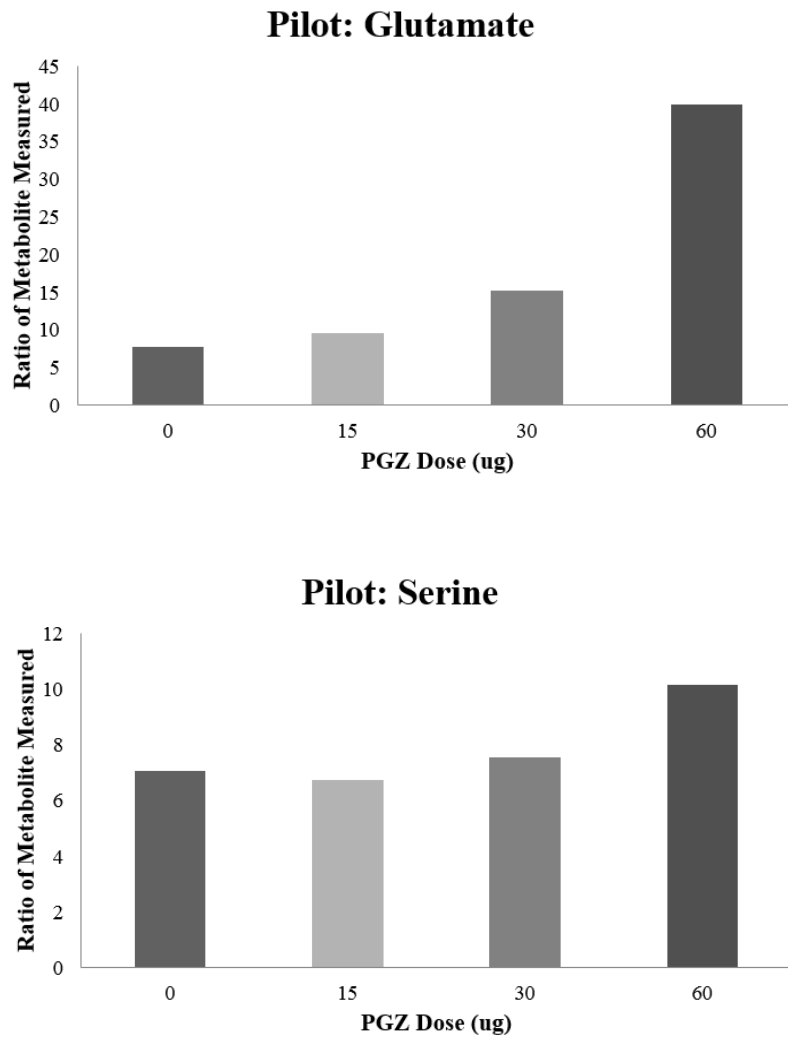


Figure 22. Glucose Metabolism. Fluxomics analysis was used to determine the ratio of ^{13}C labeled glucose as an indicator of glucose metabolism. The higher ratio following 60 mg PGZ indicates this dose was most effective in elevating glucose metabolism in the brain in non-transgenic mice.

Appendix B: Animal Care Training

All team members working with mice underwent the Animal Handler Training course given by Dr. Douglas Powell, a University of Maryland attending veterinarian. Dr. Angela Black, an ANSC veterinarian, also trained team members in proper handling technique and husbandry as required by the IACUC protocol (National Academy of Sciences, 2011). Tikina Smith, a Lab Animal Technologist at the UMD Central Animal Resource Facility (CARF), assisted team members in practice of the intranasal grip. Lastly, Dr. Brian Bequette trained team members in laboratory safety and proper handling of chemicals.

Mice were housed in the University of Maryland Animal Sciences (ANSC) facility with controlled temperature and humidity (Council, 2011), and were exposed to 12-hour light and dark cycles to mirror the normal light cycles of rodents (Chu, Li & Praticò, 2013). Mice were kept in plastic cages with stainless steel covers appropriate for their body weights of 20-35 g with generally 3-4 mice of the same treatment group in each (Searcy et al., 2012). The mice were relocated accordingly if they were incompatible or aggressive. Water and standard rodent chow (Envigo NIH-07 rodent diet) were provided ad libitum (B. Bequette, personal communication, December 2, 2013).

In instances of dehydration, Lixit water bottles were replaced with standard water bottles, and mice were provided sterile water gel (HydroGel) by ANSC staff. Water bottles were monitored and refilled daily by ANSC staff. Additionally, the ANSC facility experienced a pinworm outbreak during the study. Mouse diet was modified accordingly to include treatment for the outbreak (Teklad 2018S Sterilizable

Rodent Diet with fenbendazole 150 mg/kg) for a duration of nine weeks, after which the facility tested negative for pinworms.

Appendix C: Intranasal Insulin Method



Figure 23. Intranasal Grip. *Mice were held in the non-dominant hand with the thumb and middle finger gripping the scruff. This immobilized the head. The mouse was angled upwards for ease of intranasal administration. The Hamilton syringe was held in the dominant hand. The handler administered small drops of the treatment to alternating nostrils.*

Mice were acclimated to the researchers' handling and intranasal grip for two weeks prior to treatment to reduce stress on the mice. The study began once the mice were acclimated. Mice were taken out of the cage by the bases of their tails and placed on the cage top. The mice gripped the top of the cage with their paws, which allowed the handler to stretch the mouse body slightly. Then, the handler grasped the scruff of the neck and back, making sure to hold the skin tightly between the thumb

and middle finger. Handlers took great care to make sure that the mice were not held too tightly, as respiratory function could be restricted. Mice were then turned around onto their backs. This immobilized the head to allow for administration. Mice were held with the non-dominant hand at a 45-degree angle with nostrils pointing upwards. The required dose of solution was administered through slow drops in alternating nostrils using a Hamilton syringe. Rate of drops was determined based on speed and ease of drop inhalation. Time was taken between drops so the mice would not be overwhelmed. Different syringes were used for Saline, Insulin, and PGZ+Insulin. Syringes were thoroughly rinsed after each dosing session with distilled water (Hanson, Fine, Svitak & Faltsek, 2013).

Appendix D: In Depth Calculation of Intranasal PGZ Doses

The dosage for PGZ was approximately 30.6 μg per intranasal injection. Traditionally, an adult human who is prescribed PGZ is prescribed a 30 mg tablet that contains approximately 25 mg of pure PGZ. Because the brain is where 20% of glucose utilization occurs, this means that the body is in charge of 80% of glucose utilization. The mass of the brain, in both humans and mice, is 2% of the total body mass, and to design the dosage, both the brain's utilization of glucose as well as its mass proportion are relevant and must be compromised. Therefore, the dosage given to the mice was 10% of what the entire body would require because the brain is being specifically targeted in this experiment. Considering other factors such as the ratio of brain mass to body mass in both mice and humans, the surface area of the olfactory epithelium in both mice and humans, and the amount of liquid a mouse's nose can hold, it is ultimately determined that an acceptable dose of PGZ for a mouse would be 30.6 μg in a volume of 24 μL of acidic saline solution. Twenty-four μL of acidic saline solution is chosen because it is the common volume of intranasal liquid administered to a mouse model (Stein-Streilein, Guffee & Fan, 1988). Within these 24 μL of acidic saline, 120 μg of insulin will also be dissolved (Renner et al., 2012). This mixture of PGZ and insulin in an acidic saline solution was given intranasally to the mice. The drug on the market, known as "Actos," is a pill of PGZ hydrochloride, and this study used a pure laboratory sample of it in powder form. The powder was dissolved in 24 μL of acidic saline solution (Actos, 2008). Since using a TZD drug intranasally is a new experimental method, the

amount of drug that should be administered was calculated by considering a number of factors.

Appendix E: Immunohistochemistry Protocols

IHC is the application of both monoclonal and polyclonal antibodies to determine the tissue distribution of an antigen in relevant tissue (Duraiyan et al., 2012). It requires a brain biopsy, which is then incubated with the appropriate antibody and secondary antibody before being visualized with a dye. IHC is especially useful in determining the pathology of diseases because it can determine the presence of a large number of proteins, enzymes, and tissue structures (Duraiyan et al., 2012).

IHC helps to determine the progression of AD by measuring the presence of several markers. The *National Institute on Aging-Alzheimer's Association Guidelines for the Neuropathic Assessment of Alzheimer's Disease* recommends that IHC be used specifically for the identification of A β plaques and PHF-tau tangles (Montine et al., 2012). A β plaque density, PHF-tau tangle density, inflammation, and apoptosis will be observed through IHC.

Post-mortem analysis must be performed on sections of brain tissue to validate the existence and severity of AD pathology exhibited. The presence of A β plaques and phosphorylated tau tangles are used to quantify the pathological progression of AD, making them important markers to analyze when determining the effects of treatments on the progression of AD. Post-mortem testing is the primary means for collecting data about AD and the treatments used from the mouse brain samples. In recent literature regarding post-mortem analysis of AD model mice, there are many reliable methods available. The following methods were selected to

analyze the tissue samples: IHC staining with 6E10, microglia, and tau tangle assays, caspase 3/7 and 9 assays, and fluxomics analysis.

The 6E10 assay is a type of IHC procedure used to identify and quantify the amount of A β plaques present in an AD affected brain. Comparison of the quantity of plaques present in brain samples can determine differences in AD pathology between the brain samples. Brain samples stained with the 6E10 reagent are examined under a microscope and the amount of A β plaque present is quantified (Gupta et al., 2014).

Tau antibody staining can be performed to identify NFTs. Because AD is characterized by the abnormal phosphorylation of normal tau proteins, the antibodies used in IHC need to specifically target the abnormal, disease-associated epitopes. Along with NFTs and PHF-tau, IHC usually also includes neurophil threads, dystrophic neurites, and diffuse “pre-tangle” tau accumulations (Castellani, Alexiev, Phillips, Perry & Smith, 2007). Again, this method of IHC using specific PHF-tau antibodies allow for the qualitative identification of the amount of phosphorylated tau tangles in brain sections, and thus gives further information on the AD pathology present in the brain samples.

Microglia are major cellular mediators for inflammation. As previously mentioned, the inflammatory response is a key factor in the neuropathological features of AD. Microglia are found in the ramified, or resting state, and the amoeboid, or activated, state. Previous research has shown increased activated microglia in AD patients (Rodriguez et al., 2014).

Iba1 is a protein that is specifically expressed in macrophages and microglia, and is upregulated in the activation of those cells. Thus, the Iba1 antibody can be used as a marker for activated microglia activity. As per IHC procedures, the detection of the bound antibody will be evidenced by a colorimetric reaction. The fixed, sliced brain tissue can then be qualitatively identified for the Iba1 protein according to the colorimetric reaction, presenting information on the presence of activated microglia in the brain (Biocare Medical, n.d.).

Appendix F: Fluxomics Protocol

Adapted with the help of Leslie Juengst (Hachey et al., 1999).

Brain Preparation:

1. Place back half of left hemisphere of mouse brain in an Eppendorf tube
2. Add 0.8 mL of 1:1 methanol-water mixture
3. Homogenize at full speed
4. Add 0.8 mL chloroform
5. Mix on rotary mixer for 30 minutes
6. Centrifuge for 5 minutes at 13,000 rpm
7. Split aqueous supernatant into clean Eppendorf tube

Preparation of IPAc Derivatives of Hexoses:

1. Add 0.3 mL distilled water and 1 mL acetone
2. Centrifuge for 5 minutes at 13,000 rpm
3. Transfer to 4.0 mL Reacti-Vial
4. Blow samples down under gentle stream (2 psi) of N² gas with 50°C heat on Reacti-Therm until dry
5. Add 1 mL 0.38 M Sulfuric Acid in acetone and cap
6. Let stand at room temperature for 1 hour
7. Transfer to screw cap culture tube
8. Carefully neutralize with 2 mL 0.44 M Sodium Carbonate and vortex to mix
9. Add 2 mL of saturated sodium chloride and vortex to mix
10. Add 3 mL of ethyl acetate
11. Mix on Orbital Shaker for 20 minutes

12. Let sample separate into layers
13. Split supernatant into 4.0 mL Reacti-vial
14. Blow down at room temperature under gentle stream (2 psi) of N² gas until dry

Acetylation of IPAc Derivatives of Hexoses:

1. Acetylate by adding 100 μ L of 1:1 ethyl acetate:acetic anhydride
2. Cap and place on Reacti-Therm to heat at 60°C for 30 minutes

Data Collection

1. Transfer 125 μ L of sample to GC tubes
2. Run on GC-MS

Appendix G: Caspase 3 and 9

Caspases are cysteine-aspartic proteases. Proteases, which are enzymes that break down proteins, are involved in many physiological reactions in the body. The primary role of caspases is to degrade other proteins. One of the most important reactions regulated by proteases is the apoptosis signaling pathway (Lamkanfi & Kanneganti, 2010). Apoptosis is an integral part of normal cellular function as detailed previously in the literature review. Apoptosis can be analyzed by measuring caspase 3 and 9 activities (Elmore, 2007). Caspase 9 is an initiator caspase, which means that it signals an effector caspase to degrade proteins. Caspase 3 is an effector caspase that cleaves a large set of substrates and results in the characteristic hallmarks, both morphological and biochemical, of apoptosis. These include phosphatidylserine exposure, nuclear condensation and genomic DNA fragmentation (Lamkanfi & Kanneganti, 2010).

If samples are harvested at multiple time points, caspase assay results can provide considerable temporal and spatial information about caspase activation. Caspase assays are simple to run as well. They are also efficient--one relatively small sample can have enough material for analysis of multiple activities (Kaufmann et al., 2008).

Glossary

All citations are from the Medline Plus dictionary, unless otherwise noted

Medline Plus, (2012). Bethesda, MD: National Institutes of Health.

Actos: the brand name for pioglitazone

Agonist: a compound that can bind to a receptor not meant for it and start a reaction

Allele: a form of a gene at a locus

Alzheimer's Disease (AD): named after German neurologist Alois Alzheimer, Alzheimer's Disease is a disease in the late middle aged or old brain that causes memory loss and mood changes. In late stages, it seriously impairs most functions and causes neuronal degeneration and plaques in the brain.

Amyloid Precursor Protein (APP): a protein that, when cleaved, forms AB proteins*

Amyloid-Beta (A β) Protein: a protein that is the main component of plaques in AD

Amyloid: a protein mass deposited in organs and tissue under abnormal conditions like AD

Anesthetization: the process of blocking pain impulses and neurons to the brain; done to prevent discomfort during surgery or other treatment

Antibody: a protein in the immune system that is stimulated by an antigen and helps destroy it

Antigen: a foreign substance in the body that can be attacked by the immune system

* Cited in the reference list

Apolipoprotein E (APOE): a class of protein that makes a lipoprotein with a lipid

Apoptosis: the process of programmed cell death (cell “suicide”)

Assay: an analytical procedure that measures the presence or amount of a substance

Atrophy: shrinking in size and function of a body part or structure

Autosomal: characteristic of a chromosome other than a sex (X or Y) chromosome

A β oligomer (A β O): small soluble A β *

A β plaque: a lesion of brain tissue, usually in AD, made of mainly AB proteins and degenerating nerve cells

Biomarker: a biological indicator of a condition or disease

Blood Brain Barrier (BBB): a protective barrier between the brain and blood in the body and blocks access to the central nervous system by harmful molecules

c-jun N-terminal kinase (JNK): a phosphorylating protein that plays a key role in apoptosis*

Cascade: a biochemical process that occurs by a series of steps that each set off the next event

Central Nervous System (CNS): the nerves inside the brain and spinal cord responsible for behavior

Centrifuge: a machine that uses centrifugal force to separate substances with different densities

Cognitive function: conscious intellectual activity, like thinking and memory

* Cited in the reference list

Cytochrome: any of several intracellular hemoprotein respiratory pigments that are enzymes functioning in electron transport as carriers of electrons

Diabetes mellitus: a disease that can be hereditary or developed characterized by having low insulin levels or defective insulin, excessive amounts of urine, high blood sugar, and weight loss, hunger, and thirst

Diabetes: a disease characterized by having excessive amounts of urine

Differentiation: modification of unspecialized cells and tissues that leads to their final structure and function

Dimer: two molecules that are combined to form a single compound

Downstream insulin signaling pathway: the part of the insulin signaling pathway occurring after the initial insulin addition to the insulin receptor

Extraneuronal pathway: signaling outside of a neuron

Extrinsic: acting on the whole but originating from outside a part

Familial: hereditary, inherited

Gas chromatography: vaporized sample moves through a column and separates into component compounds

Glucose metabolism: the breakdown of glucose into smaller usable parts, which releases energy

Glycogen: the long-term storage form of glucose

Hippocampus: a region of the brain that stores and processes memory

Hydrophilicity: attraction to water

Hypometabolism: a condition characterized by a low metabolic rate

Immunohistochemistry: the study of life and its chemicals through the lenses of immunology

Immunoreactivity: reacting to particular antigens

Immunostaining: staining a substance by using a stained antibody against it

Insulin Receptor Substrate (IRS): a substance that bonds to an insulin receptor

Insulin Receptor: the place where insulin binds to the cell

Insulin Signaling Pathway (ISP): the process in which insulin allows glucose uptake*

Insulin: a protein hormone made in the pancreas that facilitates glucose uptake into cells, regulating blood sugar. When there is not enough insulin present, diabetes is developed.

Intranasal: entering through the nose

Intrinsic: completely within a part and originating in the part

Kinase: an enzyme that phosphorylates a substrate

Limbic system: parts of the brain that deal with emotion and motivation (includes the hippocampus)

Lipid: one of the main structural components of cells; fat; soluble in nonpolar organic solvents
Luminescence: the low-temperature emission of light created by cellular processes

Mild cognitive impairment (MCI): slight declines in conscious intellectual activity

Nasal mucosa: a moist mucous membrane that lines the nasal cavity

* Cited in the reference list

Neurofibrillary tangles: an accumulation of abnormally folded tau found in the cerebral cortex and hippocampus, especially in AD

Neuron: a nerve cell that helps transmit signals through the nervous system

Olfactory epithelium: the sheet of neurons lining the nasal cavity and associated with smell

Oxidative stress: stress on the body from damage caused by excess free radicals

PHF-Tau: phosphorylated tau (contains phosphate, PO_4^{3-})

Peripheral: outside of the brain and CNS

Peroxisome Proliferator-Activated Receptor (PPAR): transcription factor (protein that binds to DNA sequences to control gene expression) of genes that regulate lipid and glucose metabolism

Phosphoinositide: a derivative of phosphatidic acid that is found in the brain and does not contain nitrogen

Pioglitazone (PGZ): TZD in the hydrochloride form ($\text{C}_{19}\text{H}_{20}\text{N}_2\text{O}_3\text{S}\cdot\text{HCl}$)

Presenilin: a protein of cell membranes contributing to AD

Protease: any enzyme that cuts proteins

Proteolysis: the hydrolysis of peptides or proteins into simpler products

Rosiglitazone (RGZ): TZD in the maleate form ($\text{C}_{18}\text{H}_{19}\text{N}_3\text{O}_3\text{S}\cdot\text{C}_4\text{H}_4\text{O}_4$)

Saline: salt solution

Secretase: a protease that cleaves APP into $\text{A}\beta$ protein

Sporadic: occurring randomly or singly

Subiculum: a ventral extension of the hippocampus

Synapse: the space between two neurons that an impulse jumps to complete signaling

Tau: a protein in neurons that regulates their stability. Abnormal tau forms neurofibrillary tangles

Thiazolidinedione (TZD): a treatment for diabetes mellitus type II which activates PPAR γ

Type II diabetes (T2D): diabetes mellitus that is developed by insulin receptor resistance and hyperglycemia

Bibliography

- Alzheimer's Association. (2015). 2015 Alzheimer's disease facts and figures. *Alzheimer's & Dementia*, 11(3), 332–384. <http://doi.org/10.1016/j.jalz.2015.02.003>
- Alzheimer's Foundation of America. (2016, January 28). About Alzheimer's disease. Retrieved from <http://www.alzfdn.org/AboutAlzheimers/symptoms.html>
- American Psychiatric Association. (2013). *Diagnostic and statistical manual of mental disorders (5th ed.)*. Retrieved from <http://dx.doi.org/10.1176/appi.books.9780890425596.dsm17>
- Andersen, M. H., Becker, J. C., & Straten, P. T. (2005). Regulators of apoptosis: Suitable targets for immune therapy of cancer. *PubMed*, 4(5), 399–409.
- Banks, W., Owen, J., & Erickson, M. (2012). Insulin in the brain: There and back again. *Pharmacology & Therapeutics*, 136(1), 82–93. <http://doi.org/10.1016/j.pharmthera.2012.07.006>
- Benedict, C., Hallschmid, M., Hatke, A., Schultes, B., Fehm, H., Born, J., & Kern, W. (2004). Intranasal insulin improves memory in humans. *Psychoneuroendocrinology*, 29(10), 1326–1334. Retrieved from <http://www.ncbi.nlm.nih.gov/pubmed/15288712>
- Berg, J. M., Tymoczko, J. L., & Stryer, L. (2002). Each organ has a unique metabolic profile. In *Biochemistry* (5th ed.). New York: W H Freeman.
- Bingham, E., Hopkins, D., Smith, D., Pernet, A., Hallett, W., Reed, L., ... Amiel, S. (2002). The role of insulin in human brain glucose metabolism: An 18fluoro-deoxyglucose positron emission tomography study. *Diabetes*, 51(12), 3384–3390. <http://doi.org/10.2337/diabetes.51.12.3384>
- Blázquez, G., Cañete, T., Tobeña, A., Giménez-Llort, L., & Fernández-Teruel, A. (2014). Cognitive and emotional profiles of aged Alzheimer's disease (3 x TgAD) mice: Effects of environmental enrichment and sexual dimorphism. *Behavioural Brain Research*, 268, 185–201. <http://doi.org/10.1016/j.bbr.2014.04.008>
- Braiman, L., Alt, A., Kuroki, T., Ohba, M., Bak, A., Tennenbaum, T., & Sampson, S. R. (2001). Activation of protein kinase C zeta induces serine phosphorylation of VAMP2 in the GLUT4 compartment and increases glucose transport in skeletal muscle. *Molecular and Cellular Biology*, 21(22), 7852–7861. <http://doi.org/10.1128/MCB.21.22.7852-7861.2001>
- Brunmair, B., Staniek, K., Lehner, Z., Dey, D., Bolten, C. W., Stadlbauer, K., ... Fürsinn, C. (2011). Lipophilicity as a determinant of thiazolidinedione action in vitro: Findings from BLX-1002, a novel compound without affinity to PPARs. *American Journal of Physiology*, 300(6), C1386–C1392. <http://doi.org/10.1152/ajpcell.00401.2010>
- Chami, B., Steel, A., De La Monte, S., & Sutherland, G. (2016). The rise and fall of insulin signaling in Alzheimer's disease. *Metabolic Brain Disease*.
- Chang, L., Chiang, S., & Saltiel, A. (2004). Insulin signaling and the regulation of glucose transport. *Molecular Medicine*, 10(7-12), 65–71. <http://doi.org/10.2119/2005-00029.Saltiel>
- Chiang, S. H., Baumann, C. A., Kanzaki, M., Thurmond, D. C., Watson, R. T., Neudauer, C. L., ... Saltiel, A. R. (2001). Insulin-stimulated GLUT4 translocation requires the

- CAP-dependent activation of TC10. *Nature*, 410(6831), 944–948. Retrieved from <http://www.ncbi.nlm.nih.gov/pubmed/11309621>
- Chin, J. (2011). Selecting a mouse model of Alzheimer's disease. *Methods in Molecular Biology*, 670, 169–189. http://doi.org/10.1007/978-1-60761-744-0_13
- Choeiri, C., Staines, W., & Messier, C. (2002). Immunohistochemical localization and quantification of glucose transporters in the mouse brain. *Neuroscience*, 111(1), 19–34. Retrieved from <http://www.ncbi.nlm.nih.gov/pubmed/11955709>
- Chu, J., Li, J. G., & Praticò, D. (2013). Zileuton improves memory deficits, amyloid and tau pathology in a mouse model of Alzheimer's disease with plaques and tangles. *PLoS One*, 8(8), e70991.
- Cipriani, G., Dolciotti, C., Picchi, L., & Bonuccelli, U. (2011). Alzheimer and his disease: A brief history. *Neurological Sciences*, 32(2), 275–279. <http://doi.org/10.1007/s10072-010-0454-7>
- Collins-Praino, L., Francis, Y., Griffith, E., Wiegman, A., Urbach, J., Lawton, A., ... Brickman, A. (2014). Soluble amyloid beta levels are elevated in the white matter of Alzheimer's patients, independent of cortical plaque severity. *Acta Neuropathologica Communications*, 2(83). <http://doi.org/10.1186/s40478-014-0083-0>
- Council, N. R. (2011). Guide for the Care and Use of Laboratory Animals. Retrieved from <http://grants.nih.gov/grants/olaw/Guide-for-the-care-and-use-of-laboratory-animals.pdf>
- Craft, S., Baker, L. D., Montine, T. J., Minoshima, S., Watson, G. S., Claxton, A., ... Gerton, B. (2012). Intranasal insulin therapy for Alzheimer disease and amnesic mild cognitive impairment: A pilot clinical trial. *Archives of Neurology*, 69(1), 29–38. <http://doi.org/10.1001/archneurol.2011.233>
- Cruts, M., Theuns, J., & Van Broeckhoven, C. (2012). Locus-specific mutation databases for neurodegenerative brain diseases. *Human Mutation*, 33, 1340–1344. <http://doi.org/10.1002/humu.22117>
- De Felice, F. G., Lourenco, M. V., & Ferreira, S. T. (2014). How does brain insulin resistance develop in Alzheimer's disease? *Alzheimer's & Dementia*, 10(11), S26–S32. <http://doi.org/10.1016/j.jalz.2013.12.004>
- De la Monte, S. M., & Wands, J. R. (2008). Alzheimer's disease is type 3 diabetes—Evidence reviewed. *Journal of Diabetes Science and Technology*, 2(6), 1101–1113. Retrieved from <http://www.ncbi.nlm.nih.gov/pmc/articles/PMC2769828/?report=classic>
- Du, J., Chang, J., Guo, S., Zhang, Q., & Wang, Z. (2009). ApoE 4 reduces the expression of Abeta degrading enzyme IDE by activating the NMDA receptor in hippocampal neurons. *Neuroscience Letters*, 464(2), 140–145. <http://doi.org/10.1016/j.neulet.2009.07.032>
- El Messari, S., Ait-Ikhlef, A., Ambroise, D. H., Penicaud, L., & Arluison, M. (2002). Expression of insulin-responsive glucose transporter GLUT4 mRNA in the rat brain and spinal cord: An in situ hybridization study. *Journal of Chemical Neuroanatomy*, 24(4), 225–242. [http://doi.org/10.1016/S0891-0618\(02\)00058-3](http://doi.org/10.1016/S0891-0618(02)00058-3)
- Fiorelli, T., Kirouac, L., & Padmanabhan, J. (2013). Altered processing of amyloid precursor protein in cells undergoing apoptosis. *PLoS ONE*, 8(2), 1–12. <http://doi.org/10.1371/journal.pone.0057979>

- Freiherr, J., Hallschmid, M., Frey, W., Brünner, Y., Chapman, C., Hölscher, C., ... Benedict, C. (2013). Intranasal insulin as a treatment for Alzheimer's disease: A review of basic research and clinical evidence. *CNS Drugs*, 27(7), 505–514.
- Frequently Asked Questions: Publication of new criteria and guidelines for Alzheimer's disease diagnosis. (2011, April). Alzheimer's Association & National Institute on Aging. Retrieved from https://www.alz.org/documents_custom/Alz_Diag_Criteria_FAQ.pdf
- George, S., Ronnback, A., Gouras, G. K., Petit, G. H., Grueninger, F., Winblad, B., ... Brundin, P. (2014). Lesion of the subiculum reduces the spread of amyloid beta pathology to interconnected brain regions in a mouse model of Alzheimer's disease. *Acta Neuropathologica Communications*, 2, 17. <http://doi.org/10.1186/2051-5960-2-17>
- Grassin-Delyle, S., Buenestado, A., Naline, E., Faisy, C., Blouquit-Laye, S., Couderc, L.-J., ... Devillier, P. (2012). Intranasal drug delivery: An efficient and non-invasive route for systemic administration (Focus on opioids). *Pharmacology & Therapeutics*, 134, 366–279.
- Griffin, J. L. (2006). The Cinderella story of metabolic profiling: Does metabolomics get to go to the functional genomics ball? *Philosophical Transactions of the Royal Society of London Series B: Biological Sciences*, 361(1465), 147–161. Retrieved from <http://www.ncbi.nlm.nih.gov/pubmed/16553314>
- Gupta, A., Lacoste, B., Pistel, P., Ingram, D., Hamel, E., Alaoui-Jamali, M., ... Schipper, H. (2014). Neurotherapeutic effects of novel HO-1 inhibitors in vitro and in a transgenic mouse model of Alzheimer's disease. *Journal of Neurochemistry*, 131, 778–790. <http://doi.org/doi:10.1111/jnc.12927>
- Gupta, R., & Gupta, L. K. (2012). Improvement in long term and visuo-spatial memory following chronic pioglitazone in mouse model of Alzheimer's disease. *Pharmacology, Biochemistry, and Behavior*, 102, 184–190.
- Hachey, D. L., Parsons, W. R., McKay, S., & Haymond, M. W. (1999). Quantitation of monosaccharide isotopic enrichment in physiologic fluids by electron ionization or negative chemical ionization GC/MS using Di-O-isopropylidene derivatives. *Analytical Chemistry*, 71, 4734–4739. Retrieved from <http://pubs.acs.org/doi/pdf/10.1021/ac990724x>
- Hammaker, B. G. (2014). More than a coincidence: Could Alzheimer's disease actually be type 3 diabetes? (Cover story). *Access*, 28(9), 16-18.
- Hanson, L. R., Fine, J. M., Svitak, A. L., & Faltsek, K. A. (2013). Intranasal administration of CNS therapeutics to awake mice. *Journal of Visual Experiments*, 74. <http://doi.org/10.3791/4440>
- Hardy, J., & Selkoe, D. (2002). The amyloid hypothesis of Alzheimer's disease: Progress and problems on the road to therapeutics. *Science*, 297(5580), 353–356.
- Heneka, M. T., Sastre, M., Dumitrescu-Ozimek, L., Hanke, A., Dewachter, I., Kuiperi, C., ... Landreth, G. E. (2005). Acute treatment with the PPAR γ agonist pioglitazone and ibuprofen reduces glial inflammation and A β 1–42 levels in APPV717I transgenic mice. *Brain*, 1442–1453. <http://doi.org/10.1093/brain/awh452>
- Huang, S., & Czech, M. (2007). The GLUT4 glucose transporter. *Cell Metabolism*, 5(4), 237–252. <http://doi.org/10.1016/j.cmet.2007.03.006>

- Institute for Quality and Efficiency in Health Care. (2015, January). What is inflammation? Retrieved from <http://www.ncbi.nlm.nih.gov/pubmedhealth/PMH0072482/>
- Jack, C. R. J., Albert, M., Knopman, D. S., McKhann, G. M., Sperling, R. A., Carillo, M., ... Phelps, C. H. (2011). Introduction to revised criteria for the diagnosis of Alzheimer's disease: National Institute on Aging and the Alzheimer Association workgroups. *Alzheimer's & Dementia*, 7(3), 257–262. <http://doi.org/10.1016/j.jalz.2011.03.004>
- Kim, Y. B., Ciaraldi, T. P., Kong, A., Kim, D., Chu, N., Mohideen, P., ... Kahn, B. B. (2002). Troglitazone but not metformin restores insulin-stimulated phosphoinositide 3-kinase activity and increases p110beta protein levels in skeletal muscle of type 2 diabetic subjects. *Diabetes*, 51(2), 443–448. <http://doi.org/10.2337/diabetes.51.2.443>
- Klepper, J., & Voit, T. (2002). Facilitated glucose transporter protein type 1 (GLUT1) deficiency syndrome: impaired glucose transport into brain-- A review. *European Journal of Pediatrics*, 161(6), 295–304. Retrieved from <http://www.ncbi.nlm.nih.gov/pubmed/12029447>
- Koga, S., Kojima, A., Kuwabara, S., & Yoshiyama, Y. (2014). Immunohistochemical analysis of tau phosphorylation and astroglial activation with enhanced leptin receptor expression in diet-induced obesity mouse hippocampus. *Neuroscience Letters*, 571, 11–16. <http://doi.org/10.1016/j.neulet.2014.04.028>
- Kummer, M. P., Hermes, M., Delekarte, A., Hammerschmidt, T., Kumar, S., Terwel, D., ... Heneka, M. T. (2011). Nitration of tyrosine 10 critically enhances amyloid β aggregation and plaque formation. *Neuron*, 71(5), 833–844. <http://doi.org/10.1016/j.neuron.2011.07.001>
- Kupila, A., Sipila, J., Keskinen, P., Simell, T., Knip, M., Pulkki, K., & Simell, O. (2003). Intranasally administered insulin intended for prevention of type 1 diabetes: A safety study in healthy adults. *Diabetes Metabolism Research and Reviews*, 19(5), 415–420. Retrieved from <http://onlinelibrary.wiley.com/doi/10.1002/dmrr.397/full>
- Kupriyanova, T., & Kandror, K. (1999). Akt-2 binds to Glut4-containing vesicles and phosphorylates their component proteins in response to insulin. *The Journal of Biological Chemistry*, 274, 1458–1464. <http://doi.org/10.1074/jbc.274.3.1458>
- Lee, B. H., Hsu, W. H., Liao, T. H., & Pan, T. M. (2011). The Monascus metabolite monascin against TNF- α -induced insulin resistance via suppressing PPAR- γ phosphorylation in C2C12 myotubes. *Food and Chemical Toxicology*, 49(10), 2609–2617. <http://doi.org/10.1016/j.fct.2011/07.005>
- Leibiger, I. B., Leibiger, B., & Berggren, P. O. (2008). Insulin signaling in the pancreatic β -cell. *Annual Review of Nutrition*, 28, 233–251. <http://doi.org/10.1146/annurev.nutr.28.061807.155530>
- Leonardini, A., Laviola, L., Perrini, S., Natalicchio, A., & Giorgino, F. (2009). Cross-talk between PPAR and insulin signaling and modulation of insulin sensitivity. *PPAR Research*, 2009. <http://doi.org/10.1155/2009/818945>
- Leto, D., & Saltiel, A. R. (2012). Regulation of glucose transport by insulin: Traffic control of GLUT4. *Nature Reviews Molecular Cell Biology*, 13, 383–396. <http://doi.org/10.1038/nrm3351>

- Levy, J., Zieve, D., & Ogilvie, I. (2014). PET scan. In *A.D.A.M. Medical Encyclopedia*. Atlanta: U.S. National Library of Medicine. Retrieved from <https://www.nlm.nih.gov/medlineplus/ency/article/003827.htm>
- Li X., Song D., Leng S. X. (2015). Link between type 2 diabetes and Alzheimer's disease: From epidemiology to mechanism and treatment. *Clinical Interventions in Aging, 10*, 549-560. <http://doi.org/10.2147/CIA.S74042>
- Liu, F., Wang, Y., Yan, M., Zhang, L., Pang, T., & Liao, H. (2013). Glimepiride attenuates A β production via suppressing BACE1 activity in cortical neurons. *Neuroscience Letters, 557*(B), 90–94. <http://doi.org/10.1016/j.neulet.2013.10.052>
- Liu, J., Wang, L. N., & Jia, J. P. (2015). Peroxisome proliferator-activated receptor-gamma agonists for Alzheimer's disease and amnesic mild cognitive impairment: a systematic review and meta-analysis. *Drugs & Aging, 32*(1), 57–65. <http://doi.org/10.1007/s40266-014-0228-7>
- Liu, Z., Li, T., Li, P., Wei, N., Zhao, Z., Huimin, L., ... Wei, J. (2015). The ambiguous relationship of oxidative stress, tau hyperphosphorylation, and autophagy dysfunction in Alzheimer's disease. *Oxidative Medicine and Cellular Longevity, 2015*(352723). <http://doi.org/10.1155/2015/352723>
- Maeshiba, Y., Kiyota, Y., Yamashita, K., Yoshimura, Y., Motohashi, M., & Tanayama, S. (1997). Disposition of the new antidiabetic agent pioglitazone in rats, dogs, and monkeys. *Arzneimittelforschung, 47*(1), 29–35.
- Mandrekar-Colucci, S., & Landreth, G. E. (2011). Nuclear receptors as therapeutic targets for Alzheimer's disease. *Expert Opinion Therapeutic Targets, 15*(9), 1085–1097. <http://doi.org/10.1517/14728222.2011.594043>
- Mandrekar-Colucci, S., Karlo, J. C., & Landreth, G. E. (2012). Mechanisms underlying the rapid peroxisome proliferator-activated receptor-gamma-mediated amyloid clearance and reversal of cognitive deficits in a murine model of Alzheimer's disease. *Journal of Neuroscience, 32*(30), 10117–10128. <http://doi.org/10.1523/jneurosci.5268-11.2012>
- Mandrekar, S., & Landreth, G. (2010). Microglia and inflammation in Alzheimer's disease. *CNS & Neurological Disorders - Drug Targets, 9*(2), 156–167. Retrieved from <http://www.ncbi.nlm.nih.gov/pmc/articles/PMC3653290/>
- McKnight, P., & Najab, J. (2010). Kruskal-Wallis Test. In *Corsini Encyclopedia of Psychology* (1st ed.). Retrieved from <http://onlinelibrary.wiley.com/doi/10.1002/9780470479216.corpsy0491/abstract>
- Mittal, K., & Katare, D. P. (2016). Shared links between type 2 diabetes mellitus and Alzheimer's disease: A review. *Diabetes & Metabolic Syndrome: Clinical Research & Reviews, 1*–6. <http://doi.org/10.1016/j.dsx.2016.01.021>
- Mobbs, C. V., Kow, L. M., & Yang, X. J. (2001). Brain glucose-sensing mechanisms: Ubiquitous silencing by aglycemia vs. hypothalamic neuroendocrine responses. *American Journal of Physiology: Endocrinology and Metabolism, 281*(4), E649–E654. Retrieved from <http://www.ncbi.nlm.nih.gov/pubmed/11551839>
- Monsalve, F. A., Pyarasani, R. D., Delgado-Lopez, F., & Moore-Carrasco, R. (2013). Peroxisome proliferator-activated receptor targets for the treatment of metabolic diseases. *Mediators of Inflammation, 549627*. <http://doi.org/10.1155/2013/549627>

- Moroz, N., Tong, M., Longato, L., Xu, H., & De La Monte, S. (2008). Limited Alzheimer-type neurodegeneration in experimental obesity and type 2 diabetes mellitus. *Journal of Alzheimer's Disease*, *15*(1), 29–44.
- Mosconi, L., Pupi, A., & De Leon, M. (2008). Brain glucose hypometabolism and oxidative stress in preclinical Alzheimer's disease. *Annals of the New York Academy of Sciences*, *1147*, 180–195. <http://doi.org/10.1196/annals.1427.007>
- Mudher, A., & Lovestone, S. (2002). Alzheimer's disease – do tauists and baptists finally shake hands? *Trends in Neuroscience*, *25*(1), 22–26. [http://doi.org/10.1016/S0166-2236\(00\)02031-2](http://doi.org/10.1016/S0166-2236(00)02031-2)
- National Institutes of Health. (2009, December 22). Pioglitazone. Retrieved from <https://www.ninds.nih.gov/research/parkinsonsweb/cinaps/Compound%20Dossiers/Pioglitazone%20dossier.pdf>
- National Institutes of Health. (2016, February 1). Preventing Alzheimer's disease: What do we know? Retrieved from <https://www.nia.nih.gov/alzheimers/publication/preventing-alzheimers-disease/risk-factors-alzheimers-disease>
- Neuhauser, M., & Bretz, F. (2001). Nonparametric all-pairs multiple comparisons. *Biometrical Journal*, *43*(5), 571–580. [http://doi.org/10.1002/1521-4036\(200109\)43:5<571::AID-BIMJ571>3.0.CO;2-N](http://doi.org/10.1002/1521-4036(200109)43:5<571::AID-BIMJ571>3.0.CO;2-N)
- Niittylae, T., Chaudhuri, B., Sauer, U., & Frommer, W. (2009). Comparison of quantitative metabolite imaging tools and carbon-13 techniques for fluxomics. *Methods in Molecular Biology*, *553*, 355–372. http://doi.org/10.1007/978-1-60327-563-7_19
- Oddo, S., Caccamo, A., Shepherd, J. D., Murphy, M. P., Golde, T. E., Kaye, R., ... LaFerla, F. M. (2003). Triple-transgenic model of Alzheimer's disease with plaques and tangles: Intracellular Abeta and synaptic dysfunction. *Neuron*, *39*(3), 409–421. Retrieved from <http://www.ncbi.nlm.nih.gov/pubmed/12895417>
- Peric, A., & Annaert, W. (2015). Early etiology of Alzheimer's disease: Tipping the balance toward autophagy or endosomal dysfunction? *Acta Neuropathologica*, *129*(3), 363–381. <http://doi.org/10.1007/s00401-014-1379-7>
- Perl, D. (2010). Neuropathology of Alzheimer's disease. *Mount Sinai Journal of Medicine*, *77*(1), 32–42. <http://doi.org/10.1002/msj.20157>
- Prakash, A., & Kumar, A. (2014). Role of nuclear receptor on regulation of BDNF and neuroinflammation in hippocampus of β -amyloid animal model of Alzheimer's disease. *Neurotoxicity Research*, *25*(4), 335–347. <http://doi.org/10.1007/s12640-013-9437-9>
- Reiman, E. M., Chen, K., Alexander, G. E., Caselli, R. J., Bandy, D., Osborne, D., ... Hardy, J. (2004). Functional brain abnormalities in young adults at genetic risk for late-onset Alzheimer's dementia. *Proceedings of the National Academy of Sciences of the United States of America*, *101*(1), 284–289. <http://doi.org/10.1073/pnas.2635903100>
- Renner, D. B., Svitak, A. L., Gallus, N. J., Ericson, M. E., Frey, W. H., & Hanson, L. R. (2012). Intranasal delivery of insulin via the olfactory nerve pathway. *Journal of Pharmacy and Pharmacology*, *64*(12), 1709–1714.

- Rossor, M. N., Fox, N. C., Freeborough, P. A., & Harvey, R. J. (1996). Clinical features of sporadic and familial Alzheimer's disease. *Neurodegeneration*, 5(4), 393–397. Retrieved from <http://www.sciencedirect.com/science/article/pii/S1055833096900525>
- Rubio-Perez, J. M., & Morillas-Ruiz, J. M. (2012). A review: Inflammatory process in Alzheimer's disease, role of cytokines. *Scientific World Journal*, 756357. <http://doi.org/10.1100/2012/756357>
- Ryan, N., & Rossor, M. (2010). Correlating familial Alzheimer's disease gene mutations with clinical phenotype. *Biomarkers in Medicine*, 4(1), 99–112. <http://doi.org/10.2217/bmm.09.92>
- Sancheti, H., Patil, I., Kanamori, K., Diaz Benton, R., Zhang, W., Lin, A., & Cadenas, E. (2014). Hypermetabolic state in the 7-month-old triple transgenic mouse model of Alzheimer's disease and the effect of lipoic acid: a ¹³C-NMR study. *Journal of Cerebral Blood Flow & Metabolism*, 34(11), 1749–60. <http://doi.org/10.1038/jcbfm.2014.137>
- Santi S. D., De Leon, M. J., Rusinek, H., Convit, A., Tarshish, C. Y., Roche, A., ... Kandil, E. (2001). Hippocampal formation glucose metabolism and volume losses in MCI and AD. *Neurobiology of Aging*, 22(4), 529–539. [http://doi.org/10.1016/S0197-4580\(01\)00230-5](http://doi.org/10.1016/S0197-4580(01)00230-5)
- Sartorius, T., Peter, A., Heni, M., Maetzler, W., Fritsche, A., Haring, H. U., & Hennige, A. M. (2015). The brain response to peripheral insulin declines with age: A contribution of the blood-brain barrier? *PLOS One*, 10(5). <http://doi.org/10.1371/journal.pone.0126804>
- Schulinkamp, R. J., Pagano, T. C., Hung, D., & Raffa, R. B. (2000). Insulin receptors and insulin action in the brain: Review and clinical implications. *Neuroscience and Biobehavioral Reviews*, 24(8), 855–872. Retrieved from <http://www.ncbi.nlm.nih.gov/pubmed/11118610>
- Searcy, J. L., Phelps, J. T., Pancani, T., Kadish, I., Popovic, J., Anderson, K. L., ... Thibault, O. (2012). Long-term pioglitazone treatment improves learning and attenuates pathological markers in a mouse model of Alzheimer's disease. *Journal of Alzheimer's Disease*, 30(4), 943–961. <http://doi.org/10.3233/JAD-2012-111661>
- Sebastiao, I., Candeias, E., Santos, M., Oliveira, C., Moreira, P., & Duarte, A. (2014). Insulin as a bridge between type 2 diabetes and Alzheimer disease – How anti-diabetics could be a solution for dementia. *Frontiers in Endocrinology*, 5(110). <http://doi.org/10.3389/fendo.2014.00110>
- Shah, K., DeSilva, S., & Abbruscato, T. (2012). The role of glucose transporters in brain disease: Diabetes and Alzheimer's disease. *International Journal of Molecular Sciences*, 13(10), 12629–12655. <http://doi.org/10.3390/ijms131012629>
- Shankar, G. M., Leissring, M. A., Anthony, A., Sun, X., Spooner, E., Masliah, E., ... Walsh, D. M. (2009). Biochemical and immunohistochemical analysis of an Alzheimer's disease mouse model reveals the presence of multiple cerebral A β assembly forms throughout life. *Neurobiology of Disease*, 36(2), 293–302. <http://doi.org/10.1016/j.nbd.2009.07.021>
- Shimohama, S. (2000). Apoptosis in Alzheimer's disease—An update. *Apoptosis*, 5(1), 9–16. <http://doi.org/10.1023/A:1009625323388>
- Simpson, I. A., Dwyer, D., Malide, D., Moley, K. H., Travis, A., & Vannucci, S. J. (2008). The facilitative glucose transporter GLUT3: 20 years of distinction. *American*

- Journal of Physiology: Endocrinology and Metabolism*, 295(2), E242–E253.
<http://doi.org/10.1152/ajpendo.90388.2008>
- Small, G. W., Ercoli, L. E., Silverman, D. H. S., Huang, S.C., Komo, S., Bookheimer, S. Y., ... Phelps, M. E. (2000). Cerebral metabolic and cognitive decline in persons at genetic risk for Alzheimer's disease. *Proceedings of the National Academy of Sciences of the United States of America*, 97(11), 6037–6042. <http://doi.org/10.1073/pnas.090106797>
- Spijker, S. (2011). Dissection of rodent brain regions. In *Neuroproteomics* (Vol. 57, pp. 13–26). Springer Science and Business Media. Retrieved from http://doi.10.1007/978-1-61779-111-6_2
- Stratchen, M. W. J. (2005). Insulin and cognitive function in humans: Experimental data and therapeutic considerations. *Biochemical Society Transactions*, 33(5), 1037–1040.
- Széles, L., Töröcsik, D., & Nagy, L. (2007). PPAR γ in immunity and inflammation: Cell types and diseases. *Biochimica et Biophysica Acta: Molecular and Cell Biology of Lipids*, 1771(8), 1014–1030. <http://doi.org/10.1016/j.bbali.2007.02.005>
- Talegaonkar, S., & Mishra, P. R. (2004). Intranasal delivery: An approach to bypass the blood brain barrier. *Indian Journal of Pharmacology*, 36(3), 140–147. Retrieved from <http://www.ijp-online.com/article.asp?issn=0253-7613;year%3D2004;volume%3D36;issue%3D3;spage%3D140;epage%3D147;aulast%3DTalegaonkar>
- Tamez-Pérez, H. E., Quintanilla-Flores, D. L., Rodríguez-Gutiérrez, R., González-González, J. G., & Tamez-Peña, A. L. (2015). Steroid hyperglycemia: Prevalence, early detection and therapeutic recommendations: A narrative review. *World Journal of Diabetes*, 6(8), 1073–1081. <http://doi.org/10.4239/wjd.v6.i8.1073>
- Tong, H., Lou, K., & Wang, W. (2015). Near-infrared fluorescent probes for imaging of amyloid plaques in Alzheimer's disease. *Acta Pharmaceutica Sinica. B.*, 5(1), 25–33. <http://doi.org/10.1016/j.apsb.2014.12.006>
- Tripathi, M., & Vibha, D. (2009). Reversible dementias. *Indian Journal of Psychiatry*, 51(11), S52–S55. Retrieved from <http://www.ncbi.nlm.nih.gov/pmc/articles/PMC3038529/>
- Trippi, F. (2001). Spontaneous and induced chromosome damage in somatic cells of sporadic and familial Alzheimer's disease patients. *Mutagenesis*, 16(4), 323–327. <http://doi.org/10.1093/mutage/16.4.323>
- Turner, P., O'Connor, K., Tate, W., & Abraham, W. (2003). Roles of amyloid precursor protein and its fragments in regulating neural activity, plasticity and memory. *Progress in Neurobiology*, 70(1), 1–32. [http://doi.org/10.1016/S0301-0082\(03\)00089-3](http://doi.org/10.1016/S0301-0082(03)00089-3)
- University of Southern California. (2016). Therapeutic effects of intranasally-administered insulin in adults with amnesic Mild Cognitive Impairment (aMCI) or mild Alzheimer's disease (AD): Study of Nasal Insulin to Fight Forgetfulness (SNIFF). Retrieved from <https://clinicaltrials.gov/ct/show/NCT01767909>
- Vandal, M., White, P., Tremblay, C., St-Amour, I., Chevrier, G., Emond, V., ... Calon, F. (2014). Insulin reverses the high-fat diet-induced increase in brain A β and improves memory in an animal model of Alzheimer disease. *Diabetes*, 63(12), 4291–4301. <http://doi.org/10.2337/db14-0375>

- Wang, D., Dickson, D., & Malter, J. (2006). β -amyloid degradation and Alzheimer's disease. *Journal of Biomedicine and Biotechnology*.
<http://doi.org/10.1155/JBB/2006/58406>
- Wang, X., Perumalsamy, H., Kwon, H. W., Na, Y.-E., & Ahn, Y.-J. (2015). Effects and possible mechanisms of action of acacetin on the behavior and eye morphology of *Drosophila* models of Alzheimer's disease. *Scientific Reports*, 5(16127).
<http://doi.org/10.1038/srep16127>
- Willette, A. A., Modanlo, N., & Kapogiannis, D. (2015). Insulin resistance predicts medial temporal hypermetabolism in mild cognitive impairment conversion to Alzheimer disease. *Diabetes*, 64(6), 1933–1940. <http://doi.org/10.2337/db14-1507>
- Winkelmayer, W. C., Setoguchi, S., Levin, R., & Solomon, D. H. (2008). Comparison of cardiovascular outcomes in elderly patients with diabetes who initiated rosiglitazone vs pioglitazone therapy. *Archives of Internal Medicine*, 168(21), 2368–2375.
<http://doi.org/10.1001/archinte.168.21.2368>
- Woods, S. C., Seeley, R. J., Baskin, D. G., & Schwartz, M. W. (2003). Insulin and the blood-brain barrier. *Current Pharmaceutical Design*, 9(10), 795–800. Retrieved from <http://www.ncbi.nlm.nih.gov/pubmed/12678878>
- Xie, L., Helmerhorst, E., Taddei, K., Plewright, B., Van Bronswijk, W., & Martins, R. (2002). Alzheimer's beta-amyloid peptides compete for insulin binding to the insulin receptor. *The Journal of Neuroscience*, 22(10), RC221. Retrieved from <http://www.ncbi.nlm.nih.gov/pubmed/12006603>
- Xu, J., Zhang, R., Zuo, P., Yang, N., Ji, C., Liu, W., ... Liu, Y. (2012). Aggravation effect of isoflurane on A β 25–35-induced apoptosis and tau hyperphosphorylation in PC12 cells. *Cellular and Molecular Biology*, 32(8), 1343–1351.
<http://doi.org/10.1007/s10571-012-9860-0>
- Yin, Y., Yuan, H., Wang, C., Pattabiraman, N., Rao, M., Petell, R. G., & Glazer, R. I. (2006). 3-phosphoinositide-dependent protein kinase-1 activates the peroxisome proliferator-activated receptor-gamma and promotes adipocyte differentiation. *PubMed*, 20(2), 268–78. <http://doi.org/10.1210/me.2005-0197>
- Yoon, S., & Kim, Y. (2015). The role of immunity and neuroinflammation in genetic predisposition and pathogenesis of Alzheimer's disease. *AIMS Genetics*, 2(3), 230–249. <http://doi.org/10.3934/genet.2015.3.230>
- Zhang, H., Ma, Q., Zhang, Y., & Xu, H. (2012). Proteolytic processing of Alzheimer's β -amyloid precursor protein. *Journal of Neurochemistry*, 120, 9–21.
<http://doi.org/10.1111/j.1471-4159.2011.07519.x>
- Zolezzi, J. M., & Inestrosa, N. C. (2013). Peroxisome proliferator-activated receptors and Alzheimer's disease: hitting the blood-brain barrier. *Molecular Neurobiology*, 48(3), 438–451. <http://doi.org/10.1007/s12035-013-8435-5>
- Zou, C., Montagna, E., Shi, Y., Peters, F., Blazquez-Llorca, L., Shi, S., ... Herms, J. (2015). Intraneuronal APP and extracellular A β independently cause dendritic spine pathology in transgenic mouse models of Alzheimer's disease. *Acta Neuropathologica*, 129(6), 909–920. <http://doi.org/10.1007/s00401-015-1421-4>